UNITED NATIONS UNIVERSITY
UNU-GTP
Geothermal Training Programme

Orkustofnun, Grensasvegur 9,
IS-108 Reykjavík, Iceland

Reports 2017
Number 22

GEOTHERMAL EXPLORATION IN TINDAR AND WESTERN SIDE OF GUFUDALUR, HVERAGERDI, SW-ICELAND

Nguyen Dinh Tuan
Ministry of Natural Resources and Environment
Vietnam Institute of GeoSciences and Mineral Resources
No. 67, Chien Thang Road, Van Quan, Ha Dong
Hanoi
VIETNAM
tuan.vigmr@gmail.com

ABSTRACT

The study area of Tindar and western side of Gufudalur is a part of the Hveragerdi central volcano area, which is located on the eastern margin of the western rift zone and the western margin of the South Iceland Seismic Zone (SISZ). Hyaloclastites and lava flows dominate the lithological units in the study area. Earthquakes with epicentres in the Hveragerdi central volcano are quite common. The most recent large-size earthquakes in the SISZ happened on the 29th of May 2008 with magnitudes of 5.5 a nd then 6.3, located between the towns of Selfoss and Hveragerdi (Khodayar et al., 2008, Brandsdóttir et al., 2010). These earthquakes created new geothermal manifestations and caused an increase in geothermal activity. New surface manifestations are still forming in the study area. Geothermal activity is widely distributed in the mapped area, the main manifestations being fumaroles and steam vents, mud pools, hot, warm and cold springs, and hot, warm and steaming grounds. The manifestations are mainly controlled by faults or fractures. The major alignment of manifestations is striking in the NE-SW direction, which coincides with the direction of major faults and fractures. In addition, NW-SE, NNW-SSE and N-S oriented faults/fractures are also present and play an important role in the enhancement of geothermal activity as well as the expansion of manifestation areas.

The main purpose of this study was to map the surface manifestations, soil temperatures, and CO_2 emission measurements, and investigate the relationship between the geothermal manifestations and geological structures such as faults, fractures and lineaments. There were 365 GPS locations of geothermal manifestations taken and divided into 12 separate manifestation areas. In addition, the present result was compared to results of previous geothermal investigations done in 1995 and in 2008, soon after the earthquakes.

1. INTRODUCTION

1.1 Geology and tectonic setting of Iceland

Iceland is located in the North Atlantic Ocean at 63°23‟N to 66°30‟N. It is the surface expression of a mantle plume, which is also located at the junction between two mid-ocean ridges: the Reykjanes Ridge

(RR) in the south and the Kolbeinsey Ridge (KR) in the north (Figure 1). Each junction is an ocean-ridge discontinuity: the South Iceland Seismic Zone (SISZ) in South Iceland and the Tjörnes Fracture Zone (TFZ), or its main structure, the Húsavík-Flatey Fault (HFF), on and offshore North Iceland. Each discontinuity is marked by strike-slip faulting, normal faulting, and high seismicity. The largest earthquakes in Iceland reach magnitudes of M7.3–7.5 and they occur on strike-slip faults in these discontinuities (Gudmundsson, 2007). As such, Iceland is a part of the oceanic crust forming the floor of the Atlantic Ocean and is the subaerial part of the Iceland Basalt Plateau, which rises more than 3000 m above the surrounding sea floor and covers about 350,000 km^2. About 30 percent of the plateau (103,000 km^2) is above sea level, the remainder forms the 50-200 km wide shelf around the island, sloping gently to depths of about 400 m before cascading into the abyss (Thórdarson, 2012). In the south of Iceland, the Reykjanes Ridge comes on shore at the Reykjanes Volcanic (Rift) Zone and branches into the Western Volcanic Zone (WVZ).

Saemundsson and Einarsson (1980) and Hardarson et al. (2009) divided the geological formations in Iceland into four formations, based on age: Holocene (< 0.01 Ma); Late-Pleistocene (0.01-0.78 Ma); Plio-Pleistocene (0.78-3.3 Ma); and Tertiary (3.3-16 Ma). Icelandic rocks are mainly composed of Tertiary plateau lavas, Plio-Pleistocene lavas and hyaloclastites, formed sub-glacially, and Holocene lavas (Jóhannesson and Saemundsson, 1998, see Figure 1). According to the formation's origin, geological

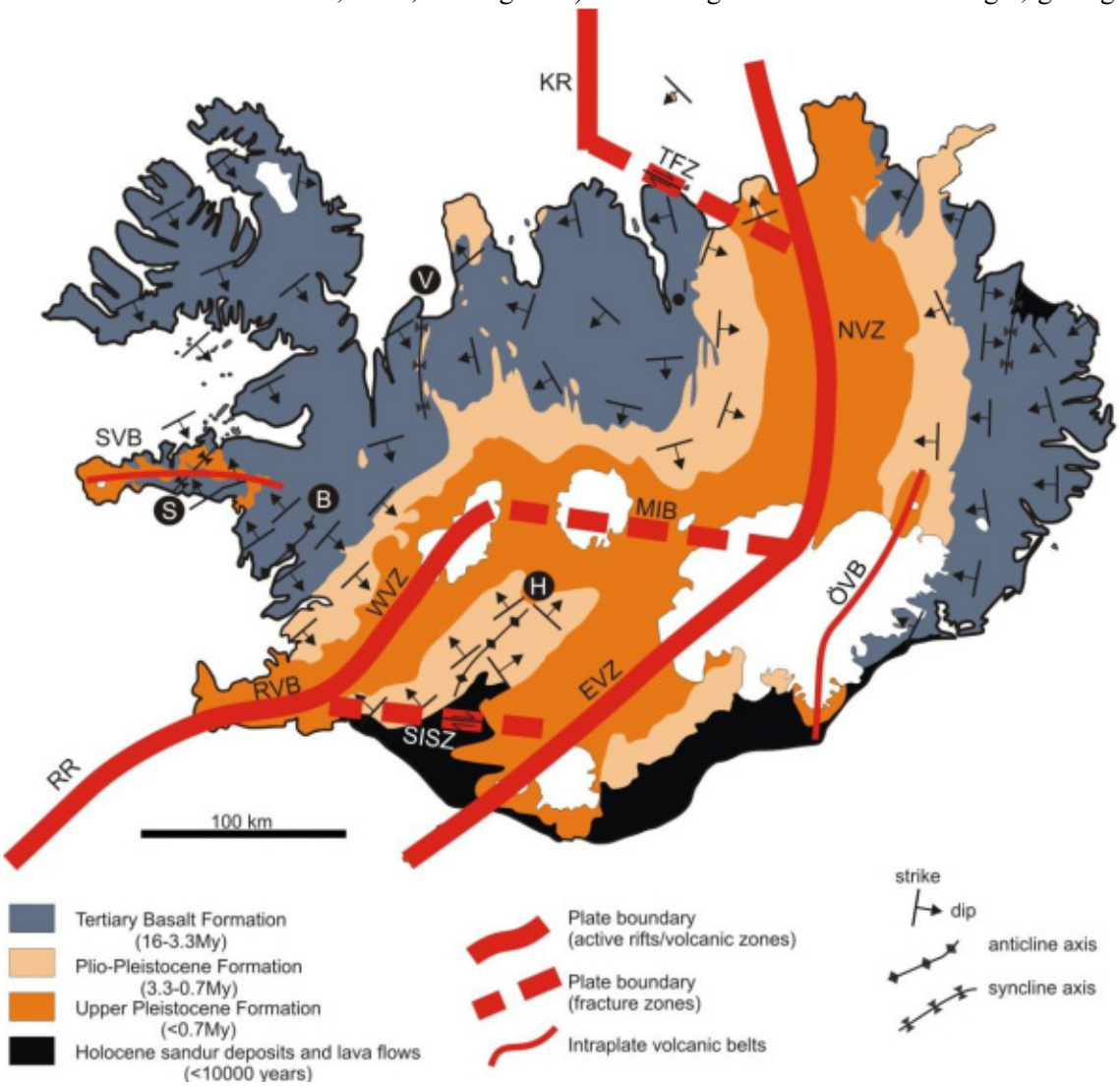

FIGURE 1: The principal elements of the geology in Iceland, outlining the distribution of the major geological subdivisions, including the main fault structures and volcanic zones and belts; relevant shortenings are explained in text above (Thórdarson, 2012)

formations in Iceland can be classified into three main types: igneous rocks (90%), consolidated sediments (10%), and intrusive and plutonic rocks (0.5%) (Jóhannesson and Saemundsson, 1998). The rocks in Iceland include three main types: basalt (75%), intermediate rocks (14%) and silicic rocks (11%) (Jakobsson et al., 2008).

1.2 Geothermal activity of Iceland

The location on the Mid-Atlantic Ridge places Iceland in the group of countries that have a large geothermal potential. A large number of volcanoes and hot springs are found in the country and earthquakes are frequent. The volcanic zone runs from the southwest to the northeast, and more than 200 volcanoes are located within this zone and at least 30 of them have erupted since the country was settled over 1100 years ago. Associated with the volcanoes are numerous geothermal systems, ranging from freshwater to saline in composition and from warm to supercritical temperatures (Ragnarsson, 2015).

Geothermal areas can be identified by surface manifestations, including hot springs, fumaroles, mud pools, while some areas may show no surface indications. Depending on their temperature, geothermal fields can be utilized in many ways from direct use to electricity generation.

Geothermal fields in Iceland are classified into high- and low-temperature fields, based on the geological setting and on temperature data from boreholes (Bödvarsson, 1961). The low-temperature areas are characterised by having temperatures less than 150°C at the depth of 1000 m, while high-temperature areas are characterised by having temperatures above 200°C at 1000 m depth (Fridleifsson, 1979).

At least 30 high-temperature areas exist within the volcanic zone with temperatures reaching more than 200°C within 1000 m depth. About 250 separate low-temperature areas with temperatures not exceeding 150°C in the uppermost 1000 m are mostly in the areas flanking the active volcanic zone. Over 600 hot spring areas (temperature over 20°C) have been located (Figure 2).

The high-temperature areas within the active rift zones are associated with active volcanoes and fissure swarms. Their heat sources are cooling intrusions or other significant magma bodies. Low-temperature areas are mainly found outside the volcanic rift zones, such as in Quaternary and Tertiary formations. They are often fracture-dominated systems, and derive their heat from hot crustal conduction with the water pushed upwards along structures such as faults, fractures and dykes. Away from the fractures, the bedrock is less permeable and heat transfer is dominated by conduction. Few Icelandic geothermal fields have reservoir temperatures in the obvious temperature gap in the definition above but those are sometimes called medium - temperature fields (Saemundsson et al., 2009).

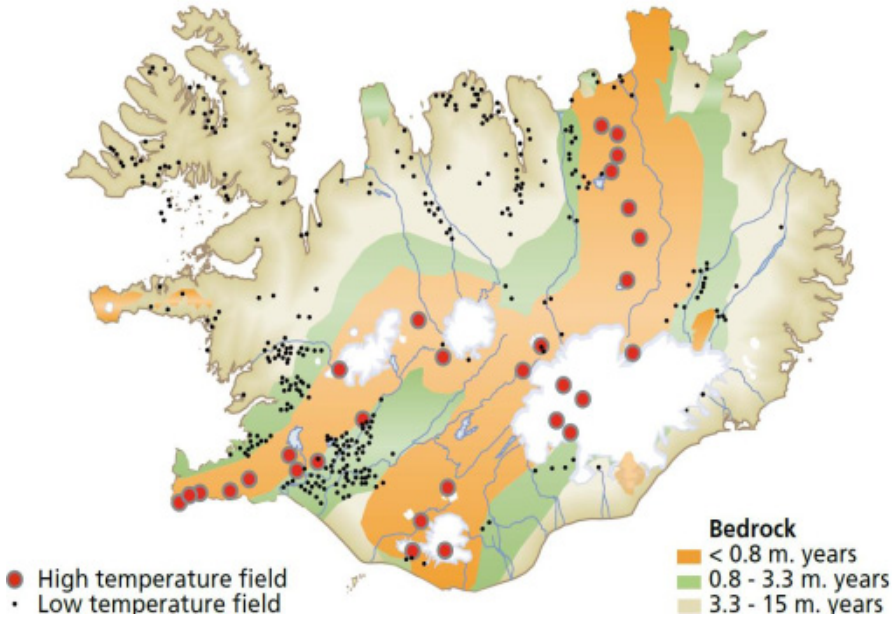

FIGURE 2: A simplified geological and geothermal map ofIceland (compiled by Saemundsson and Jóhannesson (2007), from Ragnarsson (2015))

2. GEOLOGY, TECTONIC SETTING AND GEOTHERMAL ACTIVITY OF STUDY AREA

2.1 South Iceland Seismic Zone (SISZ)

The SISZ is located at the junction of three rift segments forming a complex pattern (Figure 3). These segments are the Eastern Volcanic Zone (EVZ) and the Western Volcanic Zone (WVZ) on the northern side of the SISZ, and the Reykjanes Peninsula (RP), which forms the onland extension of the Reykjanes Ridge (Saemundsson and Fridleifsson 1992). Most of the seismic activity of the SISZ is concentrated in a zone 15-20 km wide (trending N-S) and 70 km long, trending E-W (Figure 3). However, based on the distribution of the main historical earthquake destruction areas (Einarsson and Eiríksson, 1982), and the results of recent tectonic studies in South Iceland, it is assumed that the Holocene seismic zone is as wide as 60 km (Gudmundsson, 1995).

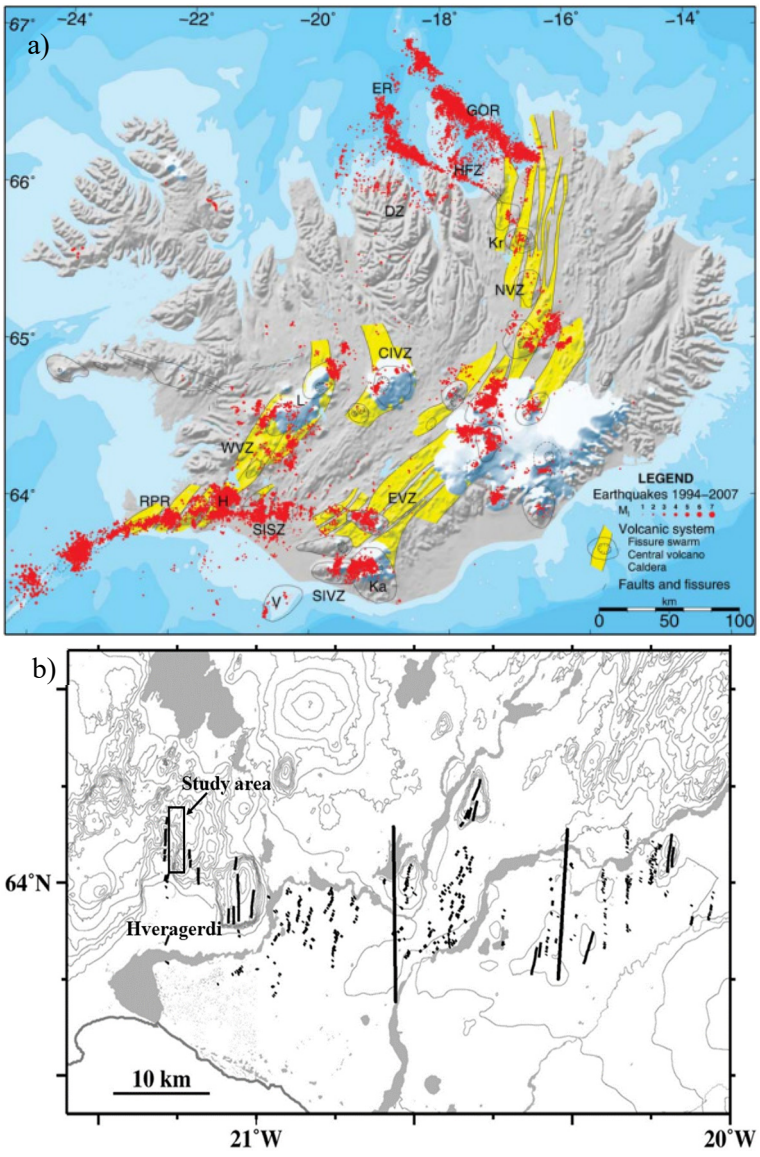

FIGURE 3: a) Earthquake epicentres 1994–2007 and volcanic systems of Iceland (Einarsson, 2008); b) Map of Holocene faults in the South Iceland Seismic Zone. The heavy N-S lines show the source faults of the June 17 and 21, 2000 earthquakes (Einarsson, 2008)

At the surface, the SISZ includes Holocene lava flows and Upper Pliocene-Pleistocene rocks. There are two main types of basaltic lavas which are named Pahoehoe and Aa, based on their surface features (Gudmundsson, 1996; Gudmundsson and Kjartansson, 1996). The Holocene lava flows are mainly basaltic Aa flows, while Pahoehoe flows, most of which are associated with shield volcanoes, are also common. The main lava flow in the area is the 8000 years old Thjórsárhraun lava flow, which covers an area of approximately 930 km^2. The longest lava stream associated with this flow is 120-140 km long and follows the channel of the river Thjórsá (latitude 64ºN) for a considerable distance. The earthquake fractures of the SISZ are most easily recognized in this lava flow, particularly in the part that follows closely latitude 64ºN (Bergerat et al, 1998).

The Pleistocene rocks are mostly hyaloclastites, sediments and tillites. Most of the hyaloclastites are basaltic breccias, which were formed in subaquatic or subglacial eruptions during periods of glaciation. However, some of them may have formed in submarine eruptions during the waning stages of the glacial periods. On the other side, one of the principal Pleistocene mountains in the area, Vördufell mountain, is mostly made of hyaloclastites topped with lava flows (Bergerat et al, 1998).

2.2 Hengill central volcano

The Hengill volcanic system lies within the western volcanic zone of Iceland, at a location where the SISZ intersects the rift zone forming a triple junction. The Hengill central volcano is the easternmost of a series of four closely spaced basaltic fissure systems that cut diagonally across the Reykjanes Peninsula. The Hengill central volcano area, which rises about 500 m above the surroundings, is intersected by a fissure swarm over 50 km long, trending N30°E and has a structure of nested grabens. In addition to the major NE-SW oriented fissure swarm, faults and hyaloclastite ridges, there are some faults and eruptive fissures transecting the centre of Hengill central volcano in a NW-SE direction through Hrómundartindur towards the Hveragerdi volcanic system, i.e. perpendicular to the main tectonic trend (Saemundsson, 1967).

The Hengill central volcanic area is commonly classified into three volcanic systems (Figure 4). The youngest and most active one is the Hengill system, which is located in the west within the axial rift zone (WVZ). The second one is the Hrómundartindur volcanic system, further to the east and much smaller in distribution. The oldest one, the Hveragerdi volcanic system, which is located furthest to the east, is extending into the area of Tindar and western Gufudalur. The oldest rocks in the whole Hengill

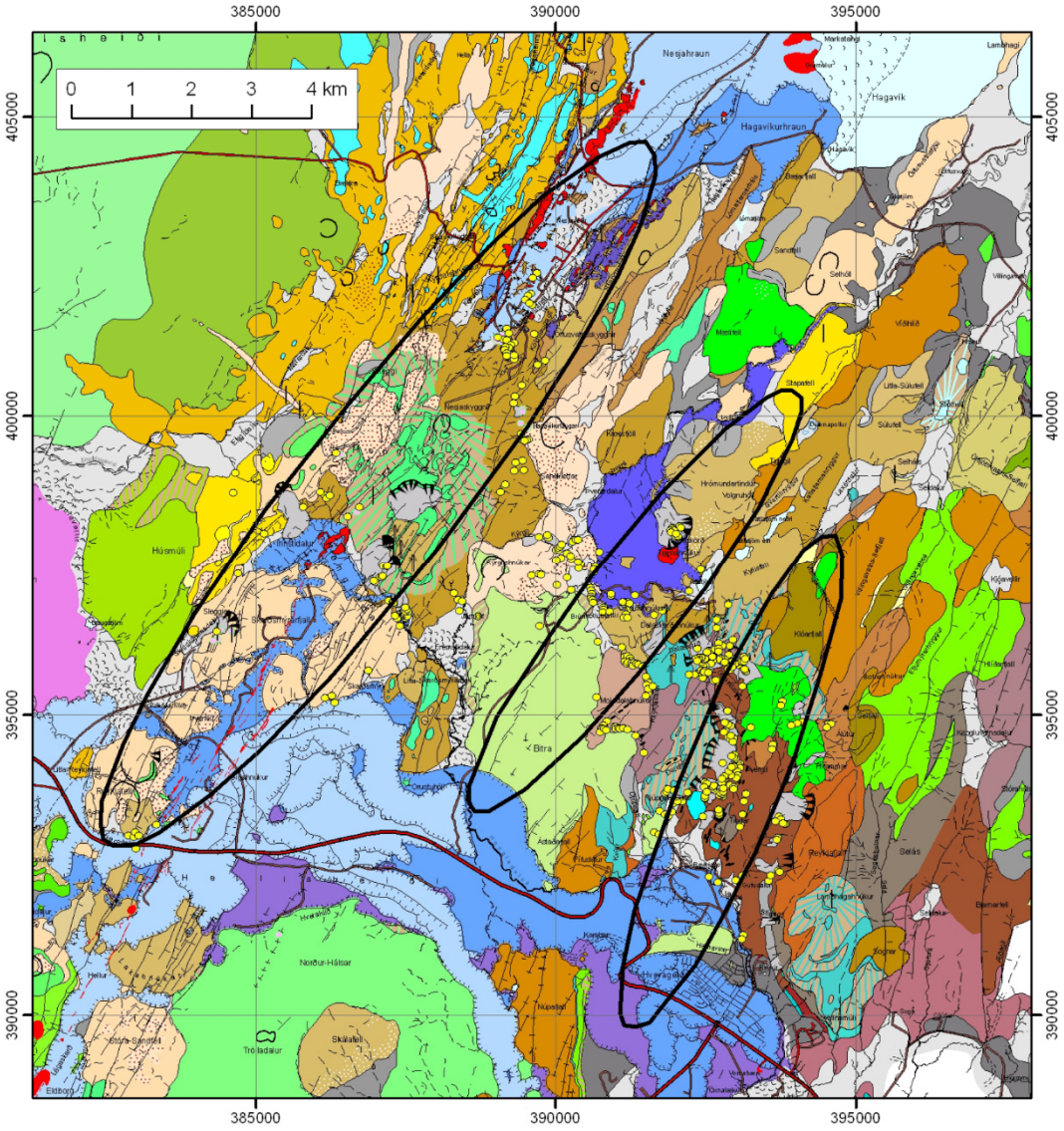

FIGURE 4: Geological map of the Hengill area, the black curves, from left to right, show the three main volcanic centres: Hengill, Hrómundartindur and Hveragerdi (Graendalur), respectively. Yellow dots denote geothermal surface manifestations (Saemundsson, 1995a)

central volcanic area, about 0.8 my old and from the Matuyama age, are located in the lowlands southeast of Hveragerdi town, and the youngest rocks are Holocene lavas, which flowed from the fissure swarm of Hengill volcano in the west (Saemundsson, 1995a).

The common volcanic forms in the Hengill area are lava shields, eruptive fissures and explosion craters formed during interglacial or postglacial times. During the glacial periods, the lava shield eruptions resulted in the building up of flat-topped mountains (tuya), while eruptive fissures formed hyaloclastite ridges. Hengill central volcano is traversed by a 10 km wide graben which runs NE-SW parallel to the hyaloclastite ridges. The western part of the Hengill area is split up by numerous subparallel normal faults. These constitute a 5 km broad inner graben of intense faulting and fissure volcanism. During postglacial times, six fissure eruptions have occurred within this graben, four south and two north of the mountain (Árnason et al., 1967). Faults and major fractures strike mostly NE-SW and are observable in the east and west, forming the boundaries of the fault and fissure zones of the volcano. During the Holocene epoch, three fissure lava eruptions were recorded approximately 9000, 5000 and 2000 years ago. The two younger NE-SW volcanic fissures are believed to provide some of the main geothermal upflow channels of the geothermal system at Hellisheidi (Franzson et al., 2005). The main rocks of the Hengill central volcano area are subglacial hyaloclastites and lavas (pillow lava and tholeiitic lava). The second most common rocks in the area are Pleistocene and postglacial lava flows (Saemundsson, 1967). From borehole data, two types of intrusive rocks have been identified: fine-grained basalt and fine-grained andesitic to rhyolitic intrusions, which are related to dykes and/or sills. The age of the Hengill central volcano was proposed to be about 0.4 million years, therefore the geothermal system must be younger (Franzson et al., 2005).

2.3 Study area and its background

The study area "Tindar and western side of Gufudalur" lies approximately four kilometres north of the town of Hveragerdi, which is located about 45 kilometres east of Reykjavík, Iceland (Figure 5). The study area is located within the Hengill and Hveragerdi (Graendalur) volcanic systems.

The volcanic rock in the study area is chiefly composed of various lithofacies of subglacially formed hyaloclastites and interglacial lava flows, to a lesser extent (Figure 6). The rock is mostly of basaltic

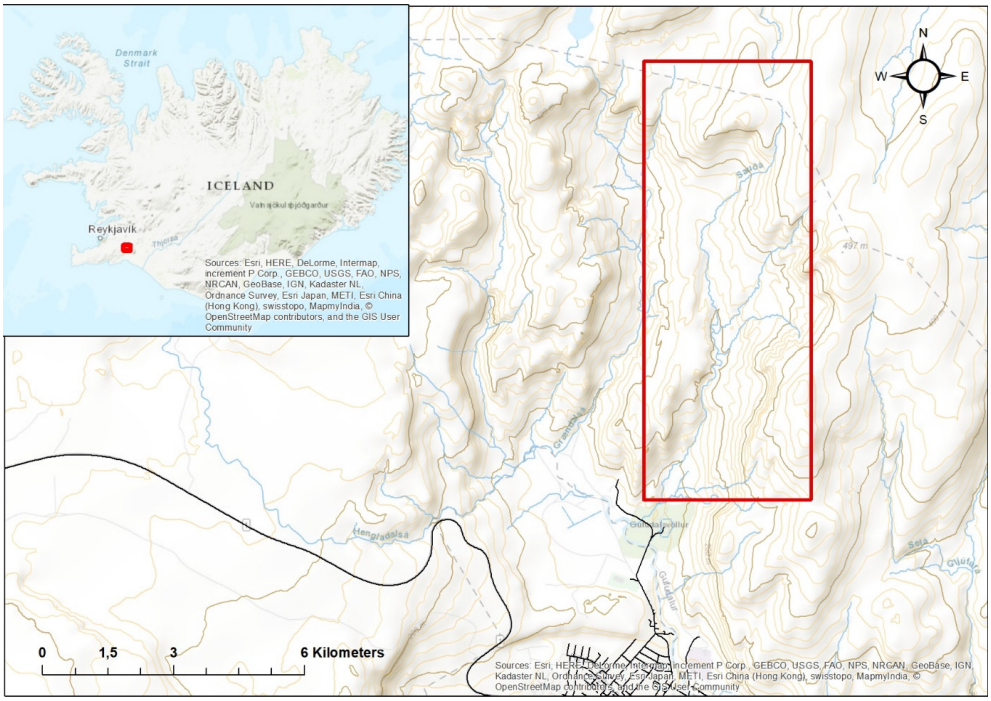

FIGURE 5: The study area - the area of Tindar Mountain and western side of Gufudalur

composition, ranging from picrite, through olivine tholeiite to tholeiites, while basaltic andesite also occurs. The hyaloclastites in the volcano form NE-SW striking ridges, the younger ones additionally showing a N-S strike. Numerous dykes are found in the centre, some of these form dyke swarms, and most of them are of the same composition as the extrusive rocks.

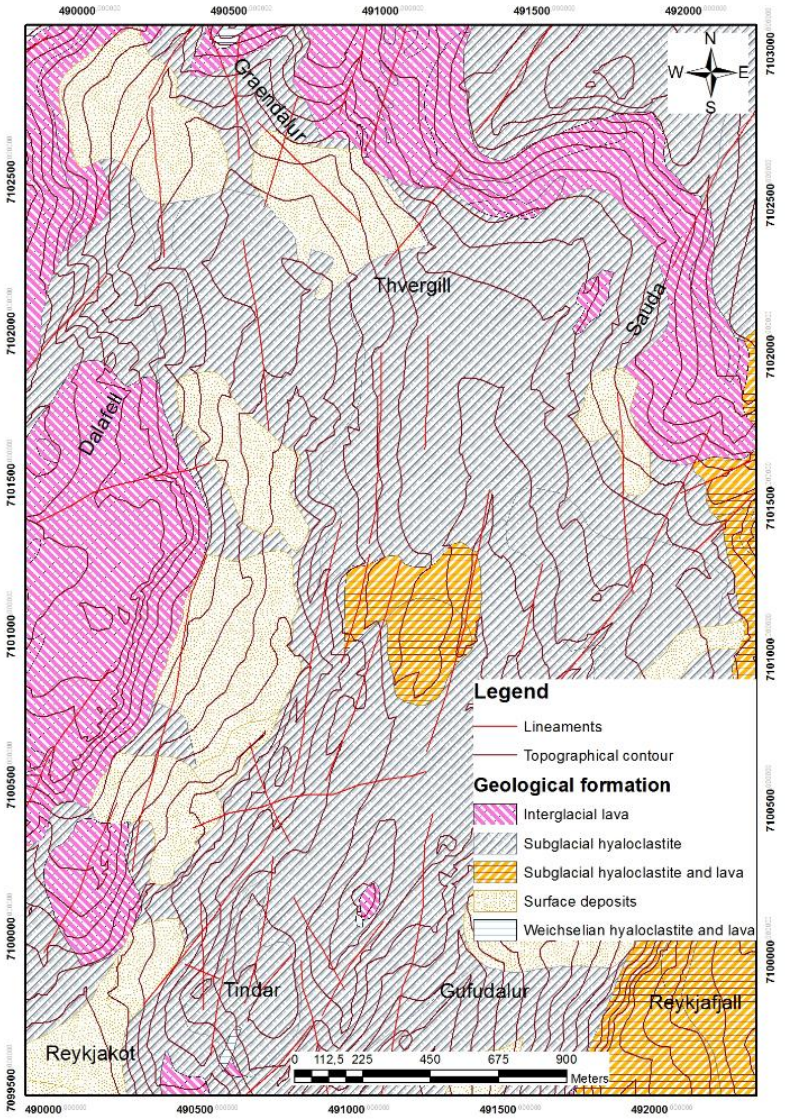

FIGURE 6: Geological map of the study area (modified from Saemundsson, 1995a)

In the study area, a sub-division can be made into two main rock series. The rocks, which have been affected by strong hydrothermal alteration are identified as the older series. The main units of these rocks are hyaloclastite of quartz tholeiite composition termed the Varmá formation, and of olivine tholeiite composition termed Tindar and Saudá formations (Saemundsson and Fridleifsson, 1992). The alteration degree reaches into the smectite/chlorite alteration zone (indicated by the pale green colour of the rocks) locally in the stratigraphically lower Varmá formation. The regional blackish to brownish colouring of the Tindar and Saudá units suggests a smectite alteration zone (Saemundsson and Fridleifsson, 1992). These rocks are also much more prominent in the study area.

The less altered rock units are categorized by a younger rock series that occurred at high elevation north of the Tindar Mount and Saudá valley, and toward Graendalsá River. The main units are a group of lavas termed the Kvíar basalts and a group of hyaloclastites higher up, extending to Mt. Reykjafjall, east of Saudá (Saemundsson and Fridleifsson, 1992).

According to previous research, the study area is situated in an active volcanic and seismic region, which gives rise to a diverse hydrothermal manifestations at the surface. The geothermal activity in this area is related to two central volcanoes, Hveragerdi and Hengill. Hveragerdi (Graendalur) central volcano is located just north of Hveragerdi, but it is older and is altered and eroded. Hengill central volcano is presently active and is located in the centre of the rift zone (Saemundsson and Arnórsson, 1971). At Hveragerdi central volcano, geothermal activities are apparent in the southern part, and in the western part, where the study area is located. The study area is characterized by many surface manifestations such as mud pools, hot grounds, fumaroles and hot springs.

With respect to the tectonic setting of Iceland, seismic activity is common in the study area. On May 29th, 2008, an earthquake of magnitude 6.3 M_w occurred in the SISZ. The epicentre was located 8 km

west-northwest of the town of Selfoss. The impact of the earthquake affected the Hveragerdi central volcano area and many sudden changes in the system were observed. Many new visible fractures formed at the surface and new fumaroles and hot springs were recorded. Many surface manifestations in the Hveragerdi geothermal field changed following the earthquake, while pressure decreases or increases caused changes in the water levels in geothermal wells in the area (Thorbjörnsson et al., 2009).

Since the earthquake occurred in 2008, several studies have been carried out in the surrounding area of Hveragerdi to record changes in the region, but few detailed geothermal mapping projects have been executed to identify changes in the Gufudalur valley within Hveragerdi central volcano.

This study focuses on observation and analysis of surface manifestations, alteration and soil temperatures, CO_2 flux through soil and correlates them with structures such as faults, fractures and lineaments.

2.4 Previous studies

The first systematic geological mapping of Gufudalur and Tindar, was carried out by Saemundsson (1967) as part of a geological survey of the Hengill area. In the 1970s, this area was mapped further in relation to drilling activities at Hveragerdi. The idea of a central volcanic succession was first published in 1971 by Saemundsson, and Arnórsson (in Saemundsson, 1979). Later, due to the combination of previous studies, the Hveragerdi central volcano area was outlined and many of the formations from which it is composed were established. In 1989, Jónsson undertook some research in the area, mostly on Upper Pleistocene and Holocene lavas (Jónsson, 1989). In 1989 and 1990, the geological mapping of this area was finished with emphasis on the lithostratigraphy, tectonics, geothermal activity and alteration (Saemundsson and Fridleifsson, 1992, 1996). The Hveragerdi central volcano was also mapped in detail by Orkustofnun, in co-operation with Hitaveita Reykjavíkur (now Orkuveita Reykjavíkur – Reykjavík Energy) (Saemundsson and Fridleifsson, 1992). These maps were later combined with the Hengill central volcano maps and published (Saemundsson, 1995a, b). In 1992, the volcano was mapped by C.L. Walker in which the eruptive units and the petrological characteristics were described. Based on surface chemical data, a conceptual model of the Hveragerdi geothermal reservoir was published by Geirsson and Arnórsson in 1995. All this work was combined in a map of the Hengill central volcano in a scale of 1:50,000 (Saemundsson, 1995a).

In 1987, a UNU Fellow (Wangombe, 1987) made a geological profile across the volcano in the Graendalur-Reykjadalur area. Geothermal exploration of the Hveragerdi - Graendalur area was carried out by UNU Fellow, Kyagulanyi (1996) with geothermal exploration of the Saudá valley west of Gufudalur was carried out by another UNU Fellow, Malik (1996). In 2003, Kristjánsson and Fridriksson published a geothermal map of the Ölfus area, partly based on research done by Saemundsson (1993a and b). Soil temperature measurements and fracture mapping in Hveragerdi were completed by Saemundsson and Kristinsson in 2005. Thorbjörnsson et al. (2009) investigated the effects of the earthquakes on 29th May 2008 on the groundwater level, geothermal activity, fractures and pressure in boreholes in the Hveragerdi area. Recently, yet another UNU Fellow, Munasinghe (2013), did a geothermal exploration in the area of Gufudalur, Hveragerdi.

3. MAPPING OF GEOTHERMAL MANIFESTATIONS AND SOIL GAS MEASUREMENTS

3.1 Methodology

The main objective of this project is mapping the surface geothermal manifestations in the study area of Tindar and western side of Gufudalur area to the north of the town of Hveragerdi. The mapping of surface manifestations involves determining the surface characteristics of the manifestations and plotting their GPS locations on a map. The geothermal mapping takes into account the spatial

representation of different types of geothermal manifestations that occur in the study area such as hot or warm springs, steam vents, mud pools, fumaroles/solfataras and hot or warm ground, silica and other encrustations, and hydrothermal alteration.

The soil temperature was measured by a digital thermometer connected by a cable to a 1 m long metallic rod fixed with a thermistor tip. The measurements were done by carefully inserting the rod into the soil to 50 cm depth except in places where the soil layer was too thin. The measuring points were tracked and recorded using GPS. The geothermal manifestations' borders and tectonic structures were also logged by GPS. The areas, where geothermal activity was observed as being clustered, are marked as active geothermal areas by giving them a location number and they will be discussed briefly. The collected data was downloaded to a computer and edited with the ArcGIS software. The final result is a geothermal map showing the temperature distribution in the valley, geothermal manifestations and tectonic structures.

The limitations of the survey included the following: Thin soil layers made it virtually impossible for the temperature probe to penetrate up to the preferred 0.5 m at some investigated locations. Some of the manifestations were located in very steep rock slopes that were unapproachable, so they were excluded. Altered grounds were also identified and mapped. Several temperature measurements were carried out to determine the temperature distribution within the hot or altered ground and special notice was given to the colour of the altered ground and its form. The precipitate's formation and its taste was recorded to distinguish between silica and other mineral salts. Samples were collected and analysed using XRD to identify the physical parameters of the rocks (permeability, porosity, and density) and alteration of minerals, which helps define zones of interest and structural features.

3.2 Characteristics of geothermal manifestations

Geothermal manifestations in the study area include hot springs, fumaroles, mud pools, hot grounds, warm grounds and clay alterations. Generally, they have the characteristics of being highly active. In the valley, manifestations such as hot springs, steam vents, mud pool and hot and warm grounds are present. At higher elevations the active geothermal manifestations present are warm and cold springs, steam vents and clay alterations. There appears to be a close relationship between the level of groundwater and geothermal manifestations in the study area.

3.2.1 Springs

Springs are quite common hydrothermal manifestations in the study area, and they have a wide range of temperatures. Based on their temperature, the springs were classified into three categories: (i) cold springs with temperatures below 15°C; (ii) warm springs with temperatures between 15 and 50°C; and (iii) hot springs with temperatures above 50°C.

A hot spring is formed by the upflow of geothermally heated groundwater (Figure 7). Silica and other mineral coatings can be observed on the rocks along the flow paths of hot springs on surface.

FIGURE 7: An example of a hot spring in the study area

3.2.2 Fumaroles/steam vents, mud pools and boiling hot springs

These forms of geothermal manifestations are generally clustered together within the same location, hence they are grouped together.

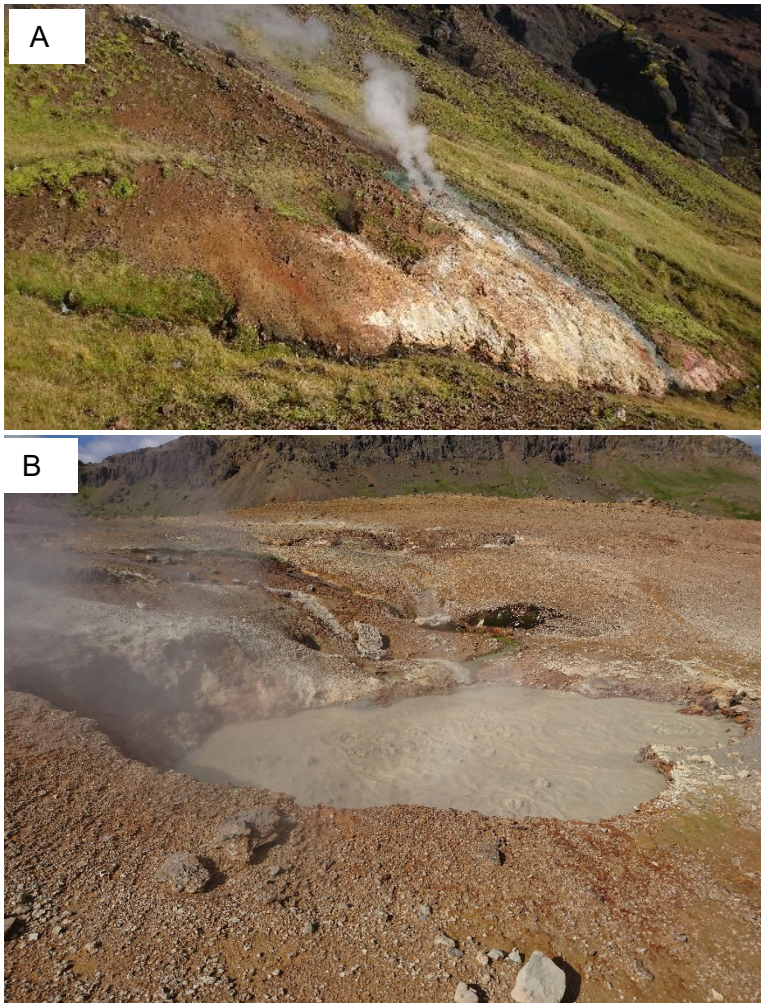

FIGURE 8: a) Fumarole in the western side of Gufudalur area; and b) Mud pool in the Tindar area

Fumaroles/steam vents are often found in active geothermal areas, emitting steam and gases such as carbon dioxide, hydrogen chloride, sulphur dioxide and hydrogen sulphide (Figure 8a). The steam is formed when hot water turns to steam as its pressure drops and subsequently emerges from the ground. Fumaroles mainly occur in hot grounds, especially in the valley floor of Graendalur or on the hill slopes where the water table is low. Most of them produce a whistling sound indicating that boiling water is at relatively shallow depths below the surface.

Mud pools are formed in high-temperature geothermal areas with a surface water deficiency. They are characterized by greyish boiling mud in a pool (Figure 8b). The viscosity of the mud usually changes along with a change in precipitation. They frequently have a halo of ferruginous earth around their margins. The collapse of the intensively altered ground around them has led to the formation of boiling mud ponds which, when filled with surface water, have temperatures of up to 90°C or at boiling point.

3.2.3 Hydrothermal alteration, minerals, salt precipitation and steaming grounds

Hydrothermal alteration is a change in the mineralogy as a result of interaction between the rock and the hot water fluids (hydrothermal fluids). The fluids carry metals in solution, either from a nearby igneous source, or from leaching out of some nearby rocks. Hydrothermal fluids cause hydrothermal alteration of rocks by hot water fluids passing through the rocks and changing their composition by adding, removing or redistributing components. The formation of these hydrothermal alteration minerals is usually dependent on the temperature, permeability, pressure, fluid composition, initial composition of the rock, and the duration of the fluid-rock interaction.

Extinct alteration, which is much more common in the study area, is characterised by white-grey clays of kaolinitie, and smectitic types. Silica and mineral salt precipitations are actively formed in areas of active geothermal zones (Figure 9). Alteration and precipitation mostly occurs along fractures within

the rock mass. The process of sintering is sometimes manifested in the form of a thin crust of mineral salts and silica, and sometimes may be accompanied by sulphur deposition (Figure 10a).

Steaming grounds are identified by yellowish green moss and dry grass (Figure 10b). Steaming grounds usually, but not always, surround the hot geothermal activity and in places where progressively more heat is being transferred and/or lost through them. The increase in temperature is usually indicated by the dying or drying of the grass. Based on their temperature, steaming grounds were classified into three categories: (i) cold grounds with temperatures below 15°C; (ii) warm grounds with temperatures between 15 and 80°C; and (iii) hot grounds with temperatures above 80°C.

FIGURE 9: Steaming ground with white silica

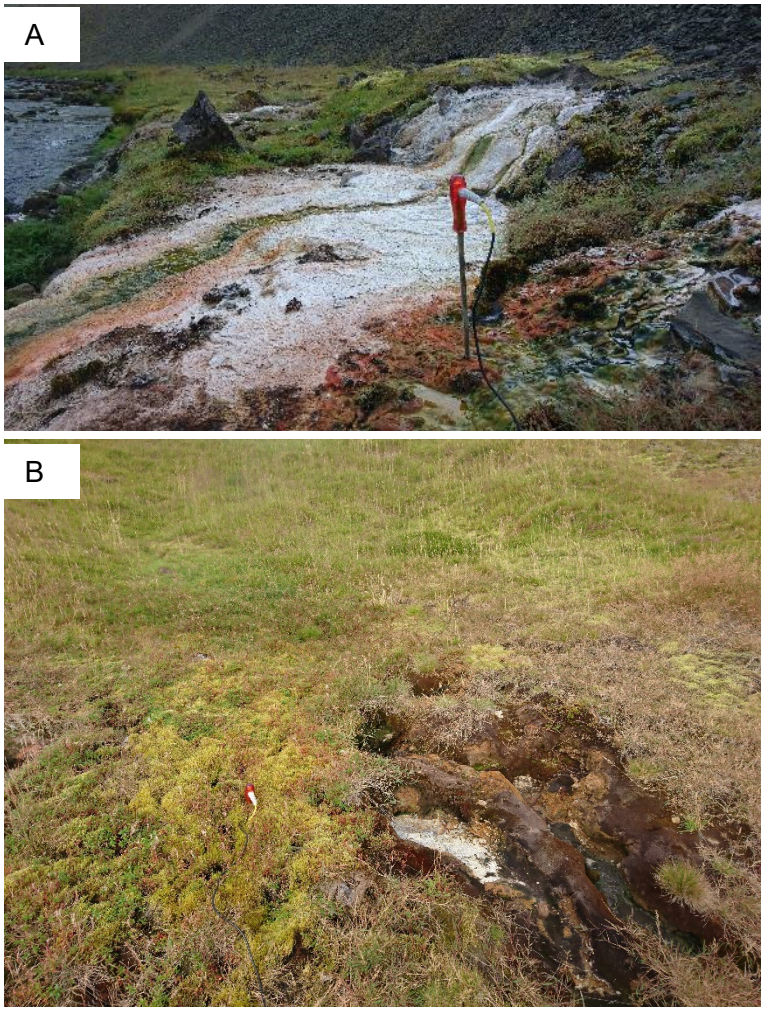

FIGURE 10: a) Alteration ground with silica and sulphur deposition; and b) Yellowish green moss and dry grass in a steaming ground

3.3 Soil gas measurements

The CO_2 flux measurements were carried out in a 800 m × 800 m grid, with 100 m between lines and measurements every 50 m on each line (Figure 11). A total of 81 measurement data points were collected by using an automated CO_2 flux meter. The flux meter is based on a closed chamber method, where a chamber with 3.06×10^{-3} m^3 total internal volume is pressed tightly on the surface and the measurement is based on the rate of CO_2 increase in the chamber. The CO_2 concentration was measured in ppm/s and displayed on a slope form on a smart phone screen which was connected to the flux meter. The shallow soil temperature measurement was also taken along with the CO_2 flux measurement at the same location and time. Both the data from CO_2 flux measurement and the soil temperature measurement were gridded along with their coordinate location by using the Golden Surfer software to create contour maps of CO_2 flux and soil temperature.

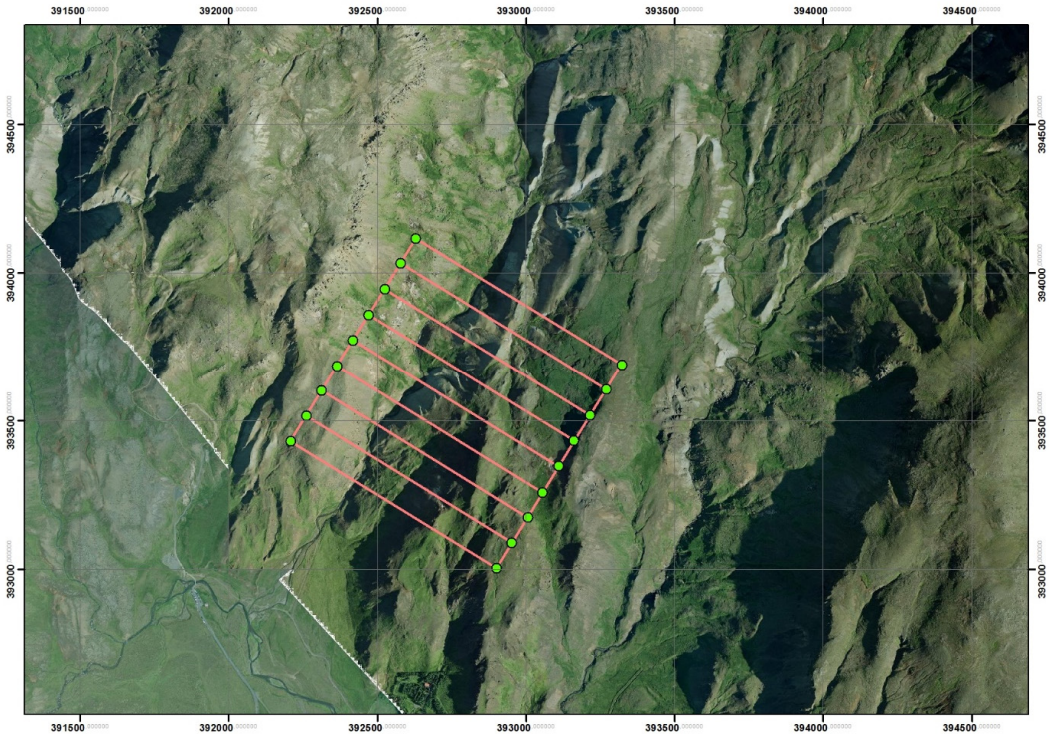

FIGURE 11: Map showing the measuring grid of the CO_2 flux and soil temperature measurements in the study area

4. RESULTS

4.1 Relationship of the surface manifestations to the geology in the study area

Geothermal manifestations such as fumaroles and hot springs are distributed from Hveragerdi area through Saudá, Tindar to the Hengill volcanic area, and transecting the main fissure swarm. The relationship between the fissures/faults and the geothermal activity is usually quite obvious, especially in relation to seismic activity. During the Holocene epoch, many changes have been observed in the surface hydrothermal activity, which are related to the seismic activity in the SISZ.

Geological structures such as faults are characterised by their horizontal or vertical displacement with the geomorphological appearance from field observation. Along the area of Tindar and western side of Gufudalur, the exposed faults are mainly with NE-SW, N-S, NNW and NW directions and show 10 to 20 m displacement. The remaining part of the area is covered by surface depositions. There, it was quite difficult to outline structural discontinuities. On the other side, geothermal manifestation are exposed in this part of the area. The alignment of geothermal manifestation is an indicator for the presence of structural discontinuities with the prominent lineaments having directional trends of the manifestations as well as being oriented similarly to faults in the study area. In addition, at intersections between two fracture systems, there is often a tendency of an increase in the intensity and expansion of the area of geothermal activity.

4.2 Details of geothermal manifestations

Geothermal manifestations in the study area mainly consist of steaming grounds, steam vents/fumaroles, hot springs, and hot grounds. Several manifestations were investigated in 1995 and were also observed after the earthquake in 2008. Figure 12 shows the map of the locations of old and present survey points of

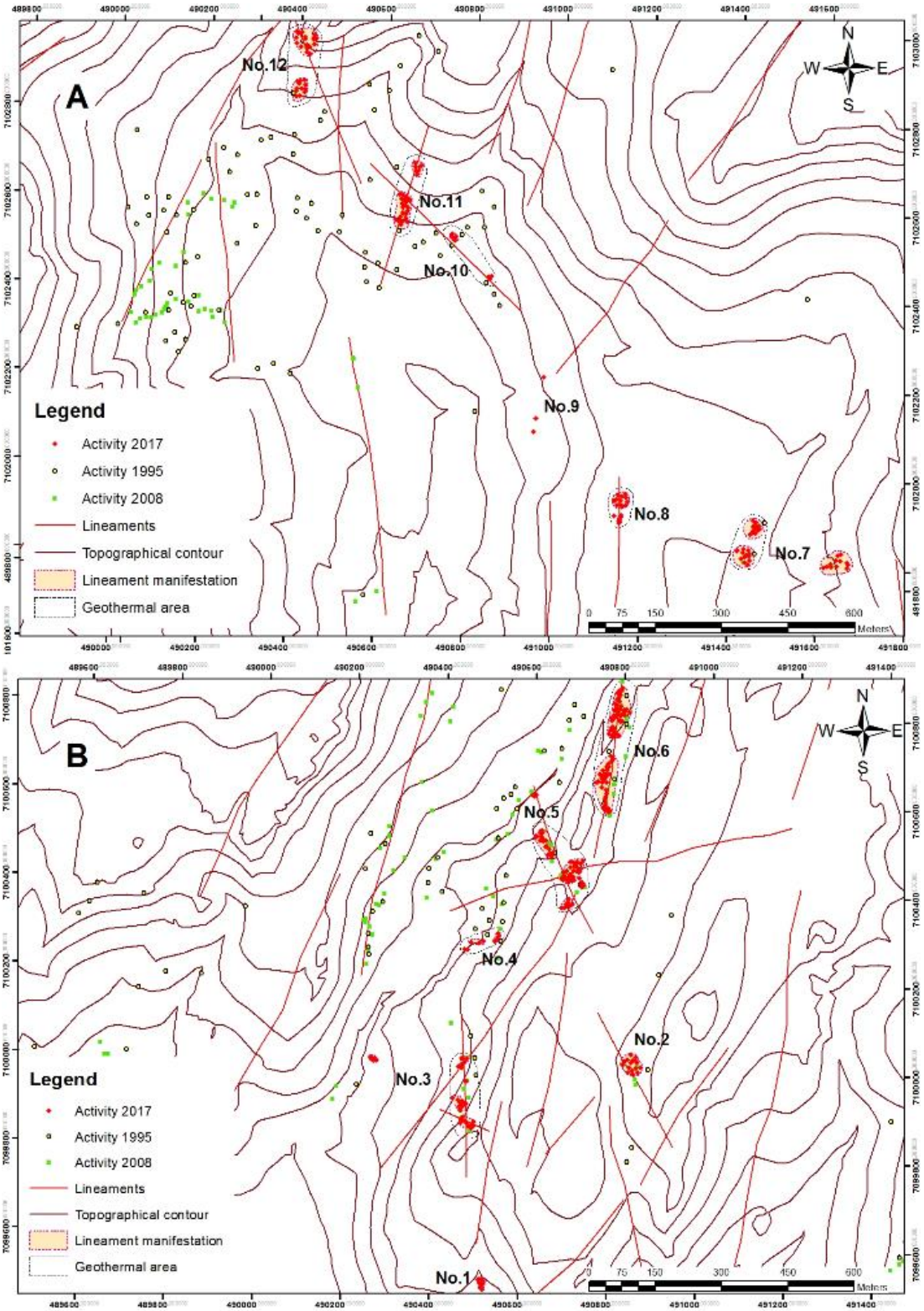

FIGURE 12: Map showing the localities of geothermal manifestations and geological structures in the area of Tindar and western side of Gufudalur, Hveragerdi; the locations of activity in 1995 and 2008 are also presented. a) Map sheet 1; b) Map sheet 2

manifestations in the study area. The geothermal manifestations, which are specifically described below, were divided into 12 localities. Among the twelve locations on the map, there are some new manifestation localities, such as: no. 1, 3a, 8, 9, and 11a, which were not identified in the previous studies. Most of the other manifestation areas, which were identified in the 1995 and 2008 investigations, displayed increasing

geothermal activity. The increasing activity can be observed at localities no. 3b, 4, 5, 6, 7, 10 and 11, while at locality no. 2 the geothermal activity seems to be stable when compared to the data from 1995 and 2008. Generally, the main alignments of the geothermal manifestations strike NE-SW, N-S, NNW-SSE and NW-SE directions, which also coincide with the directions of major faults and fractures in the study area (Figure 12).

4.2.1 Localities no. 1, 2 and 3

Figure 13 shows a detailed map of geothermal manifestations in localities no. 1, 2 and 3.

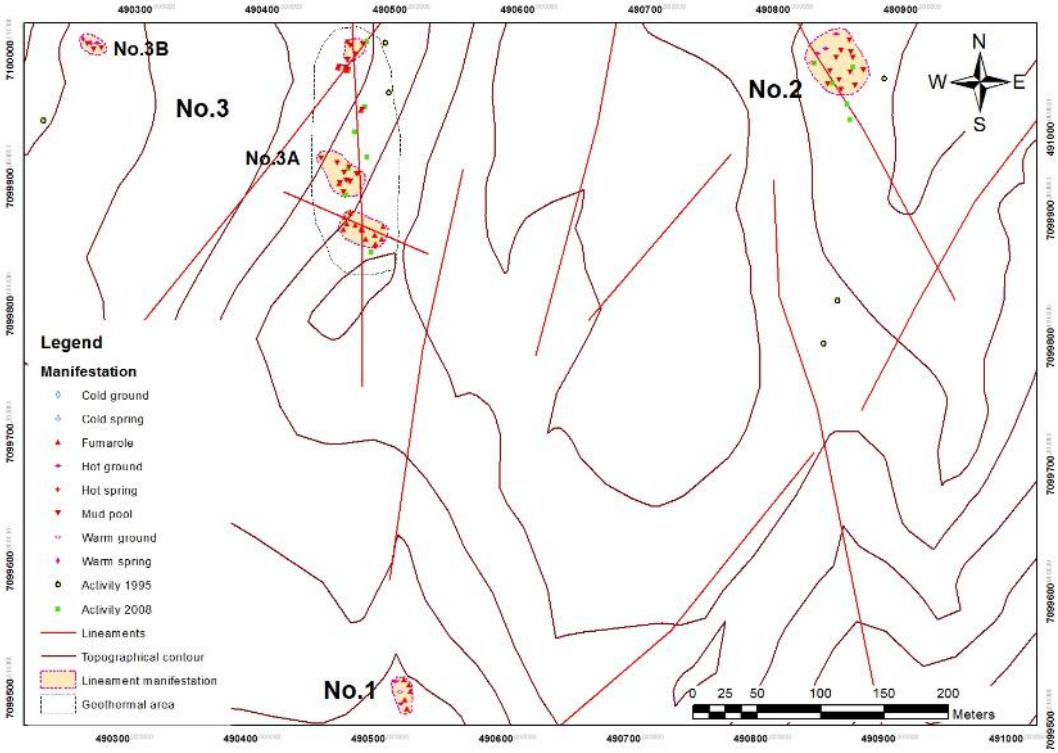

FIGURE 13: Map showing localities no. 1, 2 and 3 with geological structures; the locations of activity in 1995 and 2008 are also presented

FIGURE 14: Fumarole and steaming ground at locality no. 1

Locality no. 1: is located on the southeastern slope of the Tindar Mountain (Figure 13). The geothermal activity in this location is centred with a 1 × 1.5 m fumarole, which has a temperature of approximately 97°C, and is surrounded by steaming grounds with temperatures ranging from 33.5°C to 77°C. This manifestation is situated in a rock slide slope which is covered by yellowish green moss (Figure 14). The steaming ground is covered with white and light yellow mineral precipitates. The total area is about 30 m long and 15 m wide and extends NNE-SSW. This manifestation area was created after the investigation in 2008 and was noticed for the first time in this study.

Locality no. 2: is located on the southwestern slope, next to the top of the Tindar Mountain (Figure 13). The geothermal activity in this location was first observed in 1995, and was also investigated in 2008. Intense geothermal activity is present in this area of approximately 55 × 40 m, and consists mainly of a mud pool with surrounding steaming grounds. The mud pool, which is approximately 20 × 25 m in size, is located in the centre of the area, and the temperature ranges from 97 to 100°C, approximately. The steaming grounds are covered by white, yellow mineral precipitates. The area is surrounded by green moss and grass. According to a comparison with the previous data, the geothermal activity of this location is still increasing, which is indicated by the expansion of the manifestation area.

Locality no. 3: In this location, manifestations are divided into subareas (Figure 13). The first subarea (location no. 3A) is located on a hyaloclastite ridge, on the southwestern slope of the Tindar Mountain. The geothermal activity in 1995 and 2008 as well as in the present study, mainly consists of fumaroles and mud pools with temperatures over 95°C. There are some small mud pools with temperatures about 90-95°C located between the fumaroles and the steaming grounds (Figure 15a). The fumaroles are surrounded by steaming/warm grounds with temperatures ranging from 21 to 60°C, approximately (Figure 15b). White, yellow precipitates and mineral salts are present. One sample of precipitates, which was taken from a mud pool in this area (sample no. TU 6), was analysed by XRD and identified the presence of gypsum, anorthite and montmorillonite (smectite) (Figures 1, 2, 3 in Appendix I). The other sample of precipitates that was taken from a fumarole identified the presence of calcite and aragonite by XRD analysis (Figure 4 in Appendix I). The alignment of fumaroles and steaming grounds mainly strike in NNW-SSE direction but they are also extending in the direction of NW-SE.

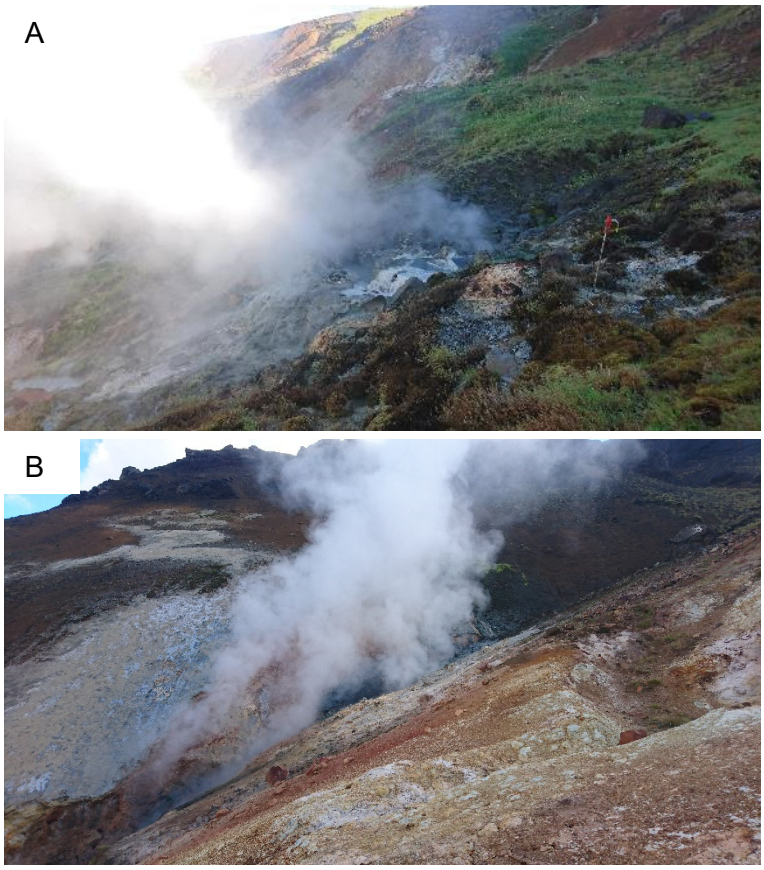

FIGURE 15: Geothermal manifestations in location no. 3A, a) Mud pool; and b) Fumarole

The second subarea of manifestation (location no. 3B) in this locality includes one recently appearing mud pool, which is located at the root of the slope, next to the left bank of the main stream of study area. This mud pool, which has temperatures ranging from 21 to 67°C, is surrounded by green moss and grass. It is extending through the NW-SE direction. The size of the mud pool is 5 m × 7 m, approximately.

4.2.2 Localities no. 4, 5 and 6

Figure 16 shows a detailed map of geothermal manifestations in localities no. 4, 5 and 6.

Locality no. 4: It is located on the northwestern slope of the Tindar Mountain, next to the left bank of the main stream in the area (Figure 16). The location consists of several altered steaming grounds, which are covered by white and yellow mineral precipitates. The temperature ranges from 37 to 98°C. The main alignment of geothermal manifestation is striking in a NE-SW direction.

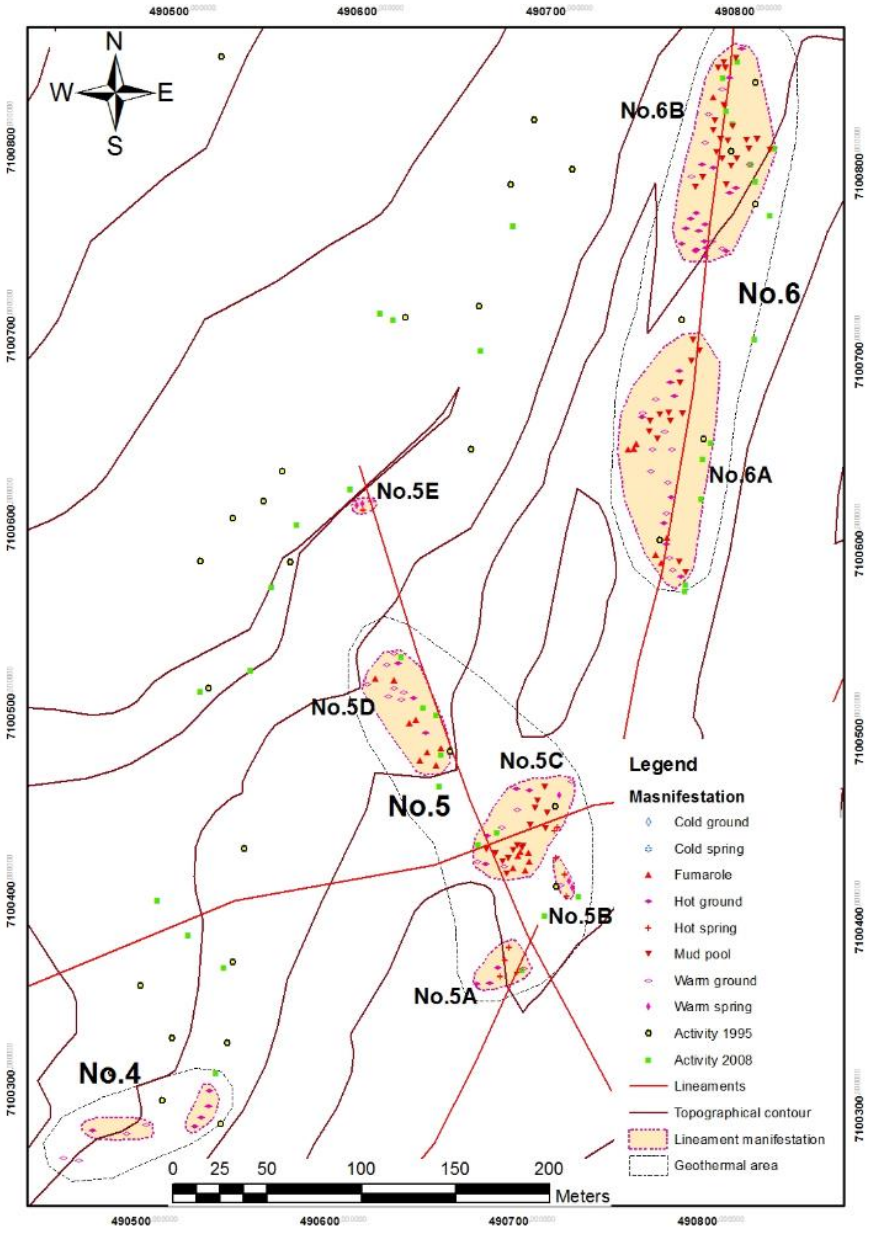

FIGURE 16: Map showing detailed geothermal manifestations in localities no. 4, 5 and 6 as well as geological structures; the locations of activities in 1995 and 2008 are also presented

Locality no. 5: It is located at the northwestern slope of the Tindar Mountain (Figure 16). The manifestations in this location consist of two hot springs and several mud pools and fumaroles, which are surrounded by steaming ground. This location was active in 1995 and is still expanding in size since the investigations in 2008, especially in NW-SE direction. Locality no. 5 is divided in to five subareas, based on the predominance of each manifestation type:

Location no. 5A consists of a warm/hot spring (Figure 17a) with temperatures approximately ranging from 73 to 86°C. The steaming grounds that surround the hot spring have even higher temperatures, from 80 to nearly 99°C, related to the effect from the adjacent fumaroles. In some places, a thin white mineral precipitate layer covers the steaming grounds and the bank of the hot spring. Vegetation around the area is mainly drying grass and moss.

Location no. 5B also consists of a hot spring with a size of 2.5 × 3.5 m. The temperature of the hot spring varies from 92 to 96°C, approximately. This hot spring is completely separate from the 5A hot spring

on the surface. White and yellow mineral precipitates cover the steaming ground that surrounds the hot spring. Temperatures of the steaming and warm grounds are from 33.5 to 56.5°C, approximately.

Location no. 5C consists of several fumaroles and mud pools (Figure 17b). The size of the fumaroles ranges from 0.3 m × 0.5 m to 0.7 m × 1 m, and of the mud pools from 0.5 m × 1 m to 1.5 m × 2 m. The temperature of the fumaroles varies from 74 to 85°C, and of the mud pool from 89.5 to 97.5°C. The surrounding steaming ground is covered by white, thin, mineral precipitates. Green moss and short drying grass are less common than in the previous two subareas. This subarea is the one with the most expansion in locality no. 5.

Location no. 5D mainly consists of fumaroles with temperatures ranging from 83.5 to 100°C (Figure 18). The size of the fumaroles is from 1 m × 1.5 m to 1.5 m × 1.6 m, approximately. The temperature of the steaming and warm grounds ranges from 30 to 96°C. White, yellow precipitates and mineral salts are present.

Location no. 5E is about 6 m long and 4 m wide, and covered by sand, gravel and pieces of rock (hyaloclastite). This subarea consists of a warm spring with a temperature range from 35.7 to 64.5°C. White and multi-coloured mineral precipitates are present and give off sulphur (H_2S) smell. Usually, subareas no. 5A, 5B, 5C, and 5D are looked at as one large geothermal manifestation area.

Locality no. 6, which is also located on the northwestern slope of the Tindar Mountain (Figure 16), lies along a small stream with northeasterly flow direction. This locality mainly consists of mud

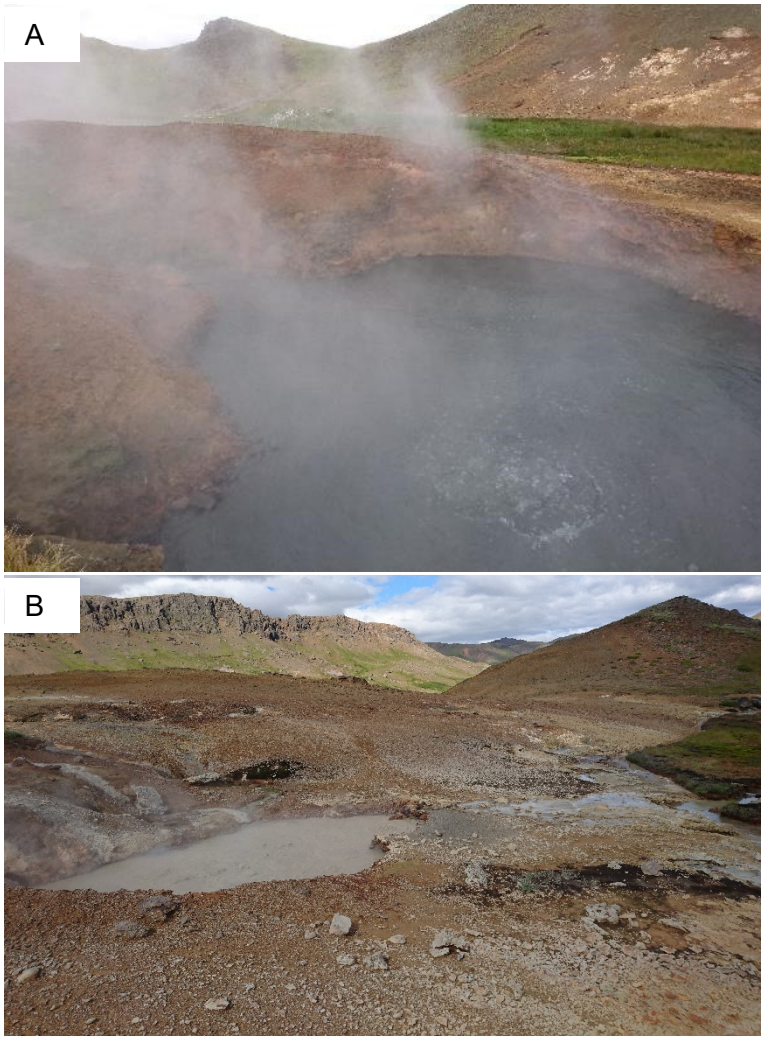

FIGURE 17: Geothermal manifestations in locality no. 5; a) Hot spring in location no. 5A;and b) Mud pool in location no. 5C

FIGURE 18: Mud pools and steaming grounds in location no. 5D

pools, steaming grounds and a few fumaroles. Based on the distribution of the manifestation, locality no. 6 is divided into two subareas.

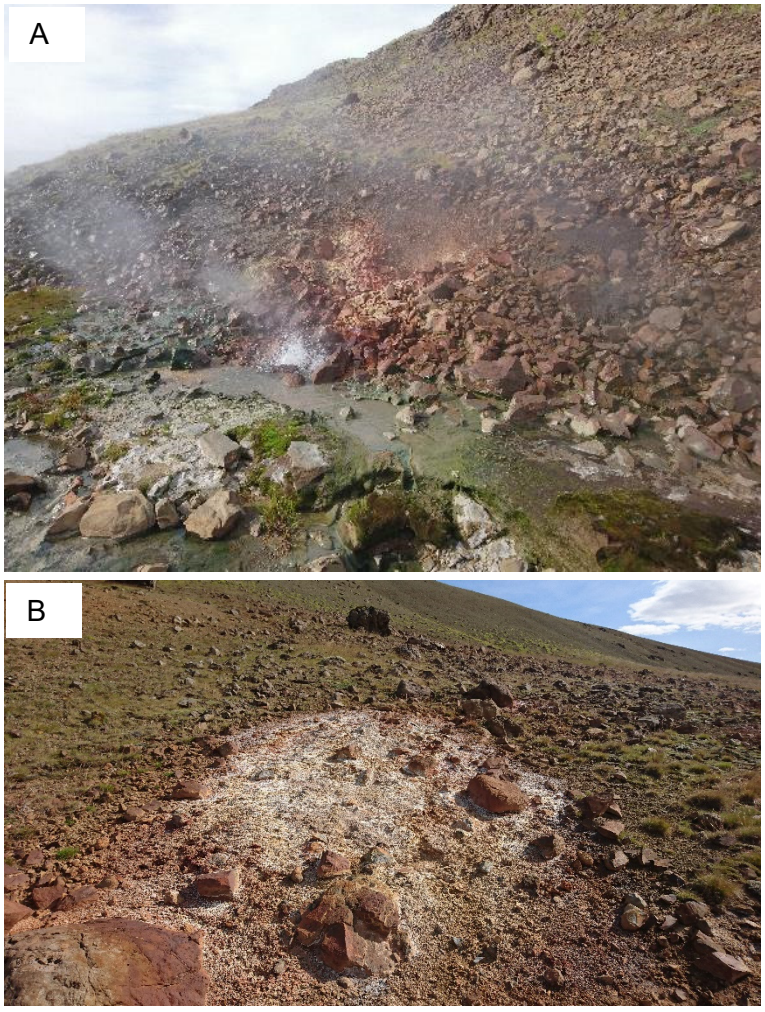

FIGURE 19: Geothermal manifestations in locality no. 6; a) Hot spring in location no. 6A; and b) Hot ground in location no. 6B

Location no. 6A consists of mud pools, steaming grounds and a few fumaroles, and hot springs. The mud pools have temperature of 99°C and sizes that range from 0.3 m × 0.4 m to 1 m × 1.5 m. The fumaroles have the average size of 0.4 m × 0.5 m and have highest temperature of 98.5°C. Steaming grounds include warm grounds and hot grounds with the temperatures ranging from 42.4 to 78.7°C and from 90.7 to 98.5°C, respectively. The hot spring has a temperature of 96.5°C (Figure 19a). Some places in the location are covered by a thin layer of white and yellow mineral precipitates. Vegetation is drying grass and yellow green moss.

Location no. 6B is 50 m northeast of location no. 6A. This location consists of mud pools, steaming grounds and a fumarole. The mud pools have a highest temperature of 99.5°C and a size that ranges from 0.5 m × 0.7 m to 1 m × 1.8 m. The fumaroles have the average size of 0.3 m × 0.5 m and have a highest temperature of 98.5°C. Steaming grounds in this location also include warm grounds and hot grounds (Figure 19b). The temperatures of warm grounds range from 46.5 to 6.7°C and of hot grounds up to 99.0°C. Vegetation is drying grass and yellow green moss, and occurs along the bank of stream only.

The two locations of 6A and 6B are usually grouped as one large geothermal manifestation area. It is also a possibility that location 6A may expand and combine with locations 5C and 5B as well.

4.2.3 Localities no. 7, 8 and 9

Figure 20 shows a detailed map of geothermal manifestations in localities no. 7, 8 and 9.

Locality no. 7 is located on the northwestern slope of the Selfjall Mountain, and was divided into two subareas (Figure 20). This area was investigated in 1995 and in 2008. Geothermal activity is still increasing, except location no. 7A, as described below. The distance between these two parts is 30 m, and there is no manifestation between them.

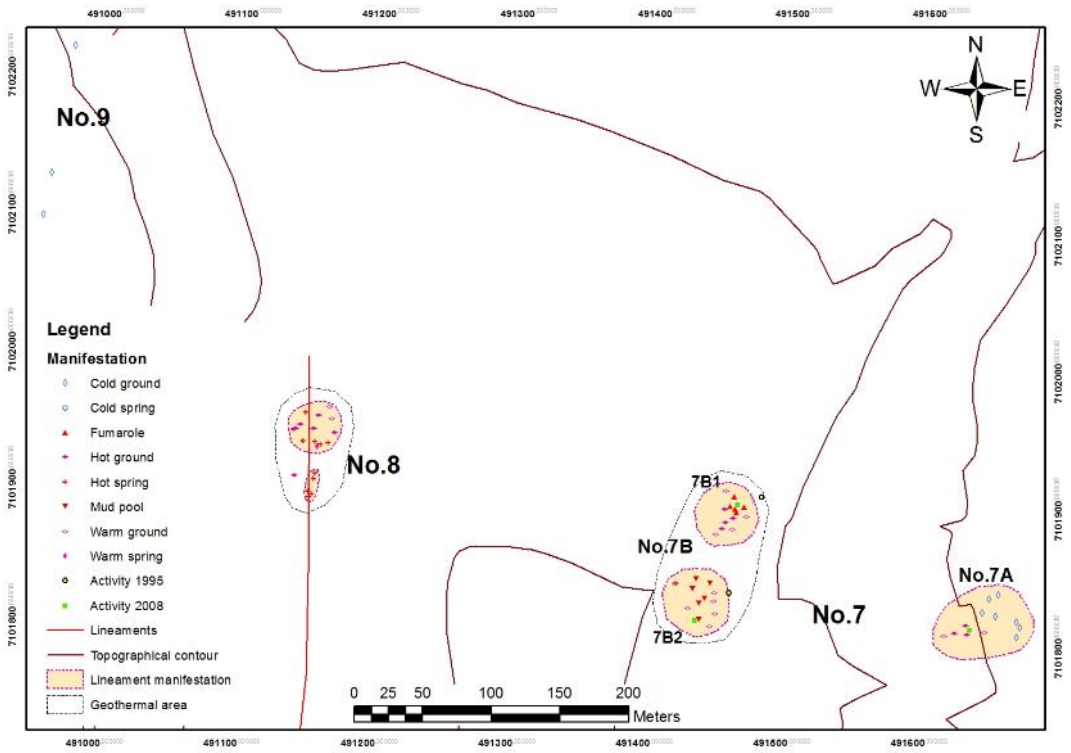

FIGURE 20: Map showing the localities of no. 7, no. 8 and no. 9 with geological structures. The locations of activity in 1995 and 2008 are also presented

Location no. 7A consist of steaming ground with a total area ~15 m long and 8 m wide (Figure 21a). This steaming ground is almost extinct with the highest measured temperature of 98°C, the average temperature is 20°C, and the lowest one is 11°C. This steaming ground is located on a diluvium slope and is covered by white, yellow mineral precipitates. Vegetation is mostly green moss.

Location no. 7B is located at the root of a diluvium slope, which is approximately 200 m east of location no. 7A. Location no. 7B1 consists of a fumarole, which is surrounded by steaming grounds. The total area is approximately 20 m long and 10 m wide, and is flanked by a small stream (direction of flow NE-SW). The temperature of the fumarole ranges from 96.5 to 98°C, while the temperature of surrounded steaming ground ranges from 51.5 to 98°C.

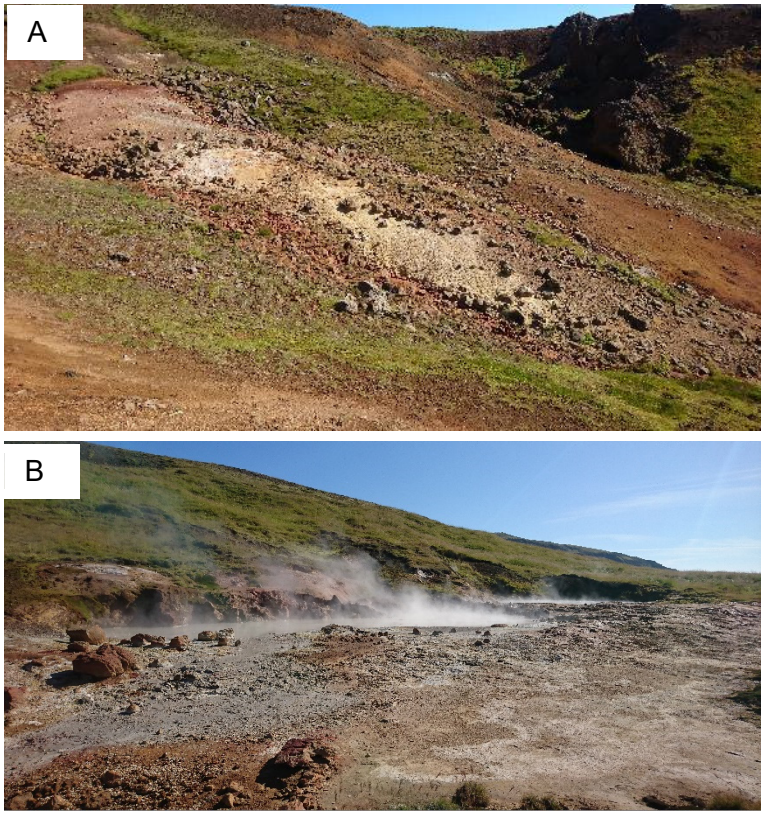

FIGURE 21: Geothermal manifestations in locality no. 7;
a) Steaming ground in location no. 7A;
and Mud pool in location no. 7B

Location no. 7B2: The total area of this location is approximately 30 m long and 20 m wide, and it is 30 m south of no. 7B1. It consists of a mud pool, which is 10 m long, and 7 m wide and steaming grounds (Figure 21b). The measured temperature of the mud pool ranges from 94 to 98°C, while the temperature of steaming grounds is from 59 to 67°C. White mineral precipitates cover the steaming ground. Vegetation is mostly drying yellow grass and drying yellow green moss.

FIGURE 22: Hot/warm springs, which are covered by grass and green moss in locality no. 8

Generally, locations No. 7B1 and 7B2 should be looked at as one larger geothermal area.

Locality no. 8 is located on the eastern bank of Klóarmelur valley (Figure 20). This location consists of several hot and warm springs and steaming grounds. The location includes two subareas that are approximately 30 m long, 25 m wide, and 20 m long and 17 m wide, respectively. The temperature of the hot springs ranges from 82 to 98°C, and of the warm springs from 44 to 74.6°C (Figure 22). The temperature of the steaming ground ranges from 66 to ~98°C. White mineral precipitates are observed. Vegetation is mostly grass and green moss. This is a recent geothermal manifestation area.

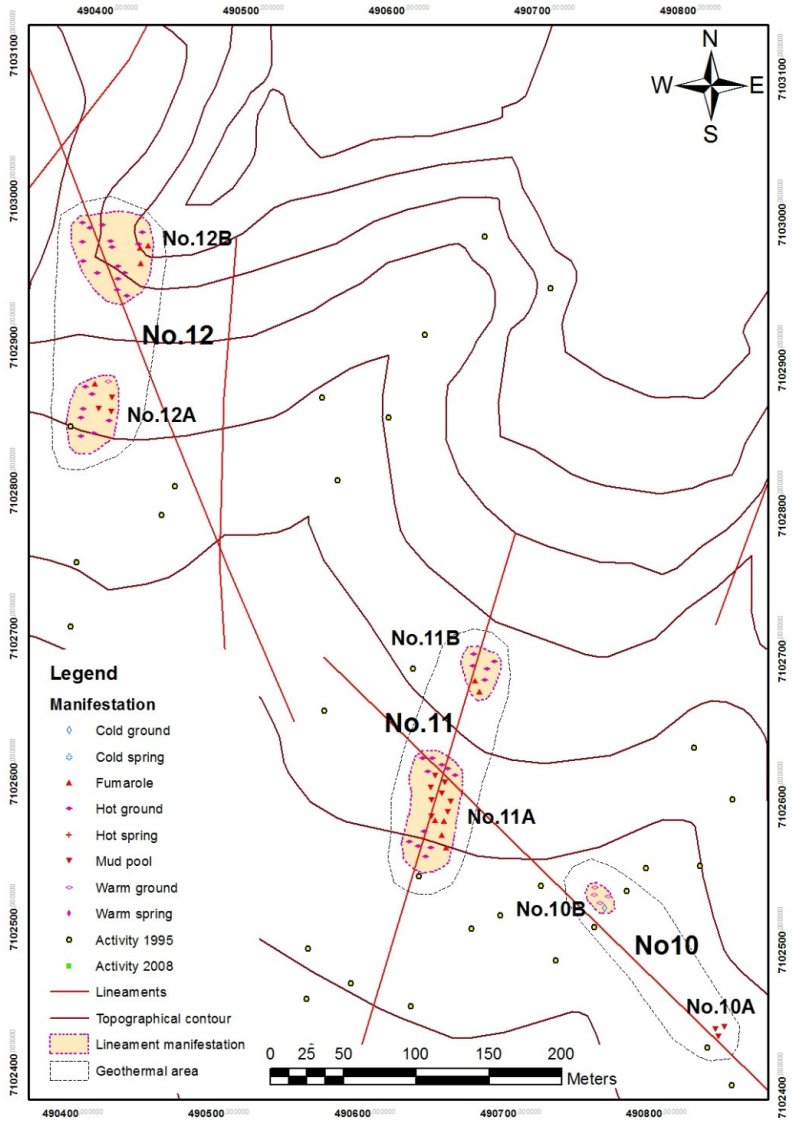

FIGURE 23: Map showing the detailed geothermal manifestations in localities no. 10, 11 and 12 with geological structures; the locations of activities in 1995 and 2008 are also presented

Locality no. 9 lies on the eastern bank of Graendalur valley (Figure 20). Geothermal manifestation in this location are presented by a few silica sinters that indicate extinct hydrothermal activity. The temperature is quite low, from 11.5 to 14°C. Vegetation at this location is green high grass with no moss.

4.2.4 Localities no. 10, 11 and 12

Figure 23 shows a detailed map of geothermal manifestations in localities no. 10, 11 and 12.

Locality no. 10 is located on the southwestern slope of the Thvergil Mountain (Figure 23). This

location was investigated in 1995, but was not surveyed in 2008. It consists of fumaroles, mud pools and steaming grounds. Based on the manifestation types, this location was divided into two subareas.

Location no. 10A consists of a mud pool, 2 m long and 1.5 m wide. This mud pool has a temperature of 77.5°C. White mineral precipitates cover the area. Vegetation in this location is a bit of drying yellow grass.

Location no. 10B is approximately 13 m long and 6 m wide, characterised by warm grounds (Figure 24). The temperature ranges from 14 to 50°C, approximately. The manifestation area is covered by a thin crust of multi-coloured mineral salts and sulphur deposition was also noticed with the smelling of sulphur (H_2S). Vegetation is mainly green grass, which is intersected by some moss.

FIGURE 24: Warm ground with a thin crust of mineral salts, covered by grass in location no. 10B

Locality no. 11 also lies on the southwestern slope of the Thvergil Mountain, and mainly consists of mud pools, steaming grounds, and fumaroles (Figure 23). Based on the manifestation types, this location was divided into two subareas: locations no. 11A and 11B, with the distance between them approximately 55 m.

FIGURE 25: Mud pool lying next to a fumarole in location no. 11A

Location no. 11A is about 110 m northwest of location no. 10A. The total area is approximately 75 m long and 35 m wide. This area consists of fumaroles and mud pools, which are intersected by warm/hot grounds (Figure 25). The size of the fumaroles varies from 0.5 m × 0.7 m to 2 m × 2,5 m, approximately, and the average temperature is 98°C. The size of the mud pools ranges from 1m x 1,3 m to 1.5 m x 1.7 m, and they have a temperature of 98°C. The temperature of warm and hot ground ranges from 38.5 to 98°C. White and yellow mineral precipitates cover the area. Brown yellow moss covers some of the hot/warm grounds. The area is surrounded by dying grass. This manifestation area is still expanding.

Location no. 11B which is approximately 30 m long and 25 m wide, and consists of fumaroles and hot grounds. The average size of fumaroles is approximately 0.3 m × 0.5 m, and the highest temperature is 98.5°C. The temperature of hot grounds also reaches 98.5°C. White mineral precipitates and green moss cover the hot grounds.

Locality no. 12 is situated on a diluvium slope at the southwestern side of the Thvergil Mountain (Figure 23) and is approximately 350 m northwest of locality no. 11. Based on the distribution of the surface manifestations, this locality is divided into two sub areas.

Location no. 12A consists of mud pools and a fumarole which are circled by hot grounds. This area has high temperatures; the mud pools have temperatures ranging from 98 to 101°C, while the hot grounds have a

temperature of 98°C. The fumarole is 0.4 m × 0.5 m in size and has a temperature of 98°C (Figure 26a). The surface of the area is covered by white mineral precipitates, fractions of rock (hyaloclastite) and green moss. This manifestation area seems to be expanding.

Location no. 12B is approximately 60 m north of location no. 12A, and consists of fumaroles and hot grounds. The fumaroles have a size range from 0.3 m × 0.5 m to 0.5 m × 0.7 m and have a highest temperature of 94.5°C. The hot grounds have temperatures that range from 82 to 90.5°C (Figure 26b). In some places, a thin, white, mineral precipitate layer covers the hot grounds and the fumaroles. Vegetation is mainly green moss.

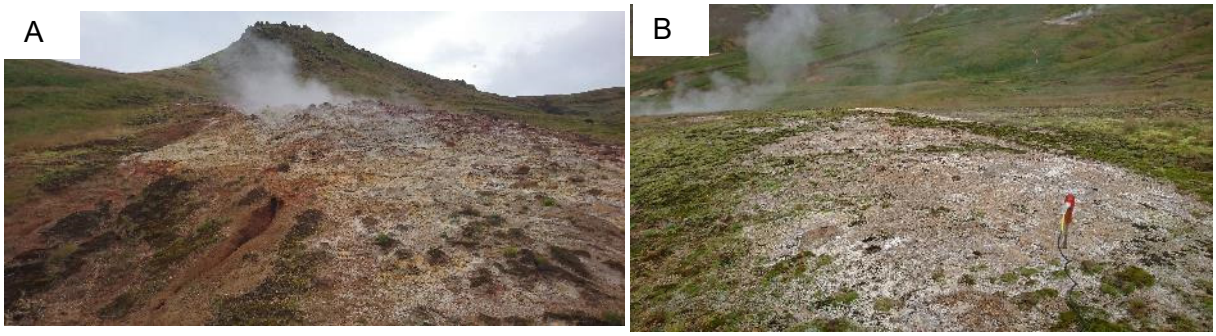

FIGURE 26: Geothermal manifestations in locality no. 12; a) Fumarole in location no. 12A; and b) Hot ground in location no. 12B

4.3 Result of CO_2 emission measurement and soil temperature map

Figure 27a shows the map of the CO_2 flux measurement, in which the darkest colour polygons indicate the highest value of emission, while in Figure 27b the brightest colour polygons indicate the highest value

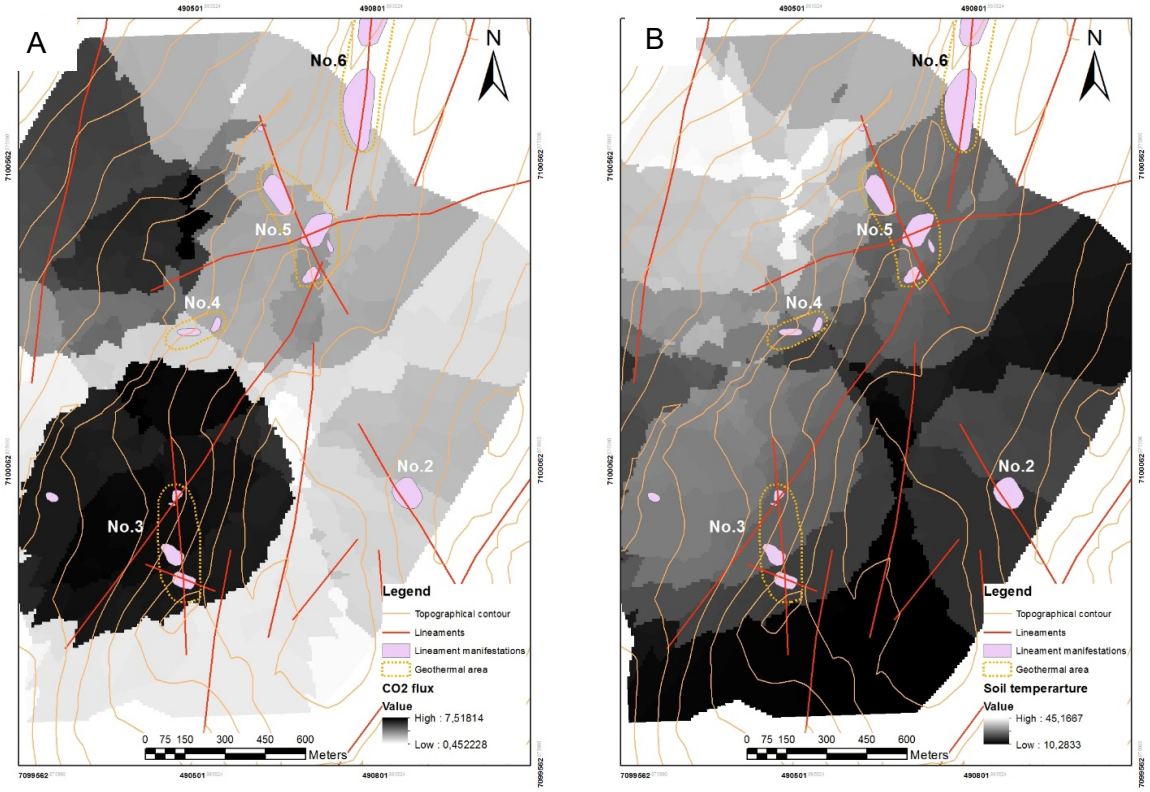

FIGURE 27: a) Map showing the result of the CO_2 flux measurements (in ppm/s); and b) Map of the soil temperature measurements (in °C)

of soil temperature. The highest value polygon of the emission coincides with the highest value polygon of soil temperature, which can be seen through the distribution of these darkest and brightest polygons. Correlating with the geological structures, generally, these results also reflect the main faults and fractures that are present in the study area.

Specifically, according to the distribution of the highest value polygons of the CO_2 flux and of the soil temperature, the NNW-SSE fracture that goes through locality no. 3 can be extended through locality no. 4 to the western area of locality no. 5. The NE-SW fracture which goes through localities no. 3 and 5 is the main fracture of this area and can be combined with the one that cuts through locality no. 6. The intersection between these two fractures form the area with the highest values of temperature and emission. The N-S fracture that is located between localities no. 2 and 3 plays no role in the activity of geothermal manifestation.

5. CONCLUSIONS

1. There were 365 GPS locations of geothermal manifestations taken which were divided into 12 separate manifestation areas. Most of the geothermal manifestations are controlled by geological structures, such as faults and fractures.

2. The major structural trends that control the geothermal manifestations are oriented NE-SW. The NW-SE, NNW-SSE and N-S oriented faults and fractures are also present and play an important role in the enhancement of geothermal activity, as well as the expansion of manifestation areas, especially when they intersect with the main fault/fracture system.

3. The distribution of high CO_2 emission and the area of highest temperature with regards to measured soil temperature mostly coincide. The results of the CO_2 flux and soil temperature measurements also indicate the effect the geological structures have on the surface manifestations, such as the NE-SW fault and NNW-SSE fracture in localities no. 3 and 4.

4. Since the earthquake on 29th of May, 2008, new geothermal areas have formed and geothermal activity has been increasing. Two new areas of manifestation have formed in the study area: Locality no. 1 and Location no. 3B. Most of the other areas were noticed as having expanded in areal size.

ACKNOWLEDGEMENTS

I would like to express my deep considerations to the Government of Iceland and the United Nations University Geothermal Training Programme for the sponsorship of this six-month training programme. I also would like to thank the Vietnam Institute of Geosciences and Mineral Resources for nominating me to attend in it.

My special gratitude also goes to Mr. Lúdvík S. Georgsson, Mr. Ingimar G. Haraldsson and Ms. Málfrídur Ómarsdóttir for their generous advice and efficient help throughout the training programme, and for assisting with the drawings and report formatting. Many thanks go to Ms. Thórhildur Ísberg and Mr. Markús A.G. Wilde for their assistance and for the training facilitation through the six months.

I would like to acknowledge my supervisor, Mr. Sigurdur G. Kristinsson, for the efforts he put into the production of this report and for critically reviewing it. I would also like to extend my special thanks to Ms. Audur A. Óladóttir, Ms. Anette K. Mortensen and Dr. Gudmundur Ómar Fridleifsson for giving me exciting geology lectures and sharing their amazing knowledge of geological field work. Also, I would

like to extend my gratitude to all of the lecturers and staff members at ÍSOR – Iceland GeoSurvey for their help and willingness to share their knowledge and experience.

I am also grateful to Mr. Tran Trong Thang, a 1996 UNU Fellow, for his encouragement and support of me participating in this course.

To Andualem, Risper and Adonias of the Geology team and to all the 2017 UNU Fellows, it was a pleasure to study and experience six months of life with you in Reykjavík, Iceland. Hope to see you again in near future.

REFERENCES

Árnason, B., Theodórsson, P., Björnsson, S., and Saemundsson, K., 1967: Hengill, a high-temperature thermal area in Iceland. *Bull. Volcanologique, XXXIII-1*, 245-260.

Bergerat, F., Gudmundsson, A., Angelier, J., and Rögnvaldsson, S.Th., 1998: Seismotectonics of the central part of the South Iceland Seismic Zone. *Tectonophysics, 298*, 319-335.

Bödvarsson, G., 1961: Physical characteristics of natural heat resources in Iceland. *Jökull, 11*, 29-38.

Brandsdóttir, B., Parsons, M., White, R.S., Gudmundsson, O., Drew, J. and Thorbjarnardóttir, B.S., 2010: The May 29th 2008 earthquake aftershock sequence within the South Iceland Seismic Zone: Fault locations and source parameters of aftershocks, 2008, *Jökull, 60,* 23-46.

Einarsson, P., 2008: Plate boundaries, rifts and transforms in Iceland. *Jökull, 58*, 35-58.

Einarsson, P., and Eiríksson, J., 1982: Earthquake fractures in the districts Land and Rangárvellir in the South Iceland Seismic Zone. *Jökull, 32*, 113-120.

Franzson, H., Kristjánsson, B.R., Gunnarsson, G., Björnsson, G., Hjartarson, A., Steingrímsson, B., Gunnlaugsson, E., and Gíslason G., 2005: The Hengill Hellisheidi geothermal field. Development of a conceptual geothermal model. *Proceedings of the World Geothermal Congress 2005, Antalya, Turkey,* CD, 7 pp.

Fridleifsson, I.B., 1979: Geothermal activity in Iceland. *Jökull, 29,* 47-56.

Geirsson, K. and Arnórsson, S., 1995: Conceptual model of the Hveragerdi geothermal reservoir based on chemical data. *Proceedings of the World Geothermal Congress 1995, Florence, Italy, 2,* 1251-1256.

Gudmundsson, A.T, 1995: Ocean-ridge discontinuities in Iceland. *J. Geological Society, London, 152*, 1011-1015.

Gudmundsson, A.T, 1996: *Volcanoes in Iceland*. Vaka-Helgafell, Reykjavík, 136 pp.

Gudmundsson A.T, 2007: Infrastructure and evolution of ocean-ridge discontinuities in Iceland. *J. Geodynamics, 43-1,* 6-29.

Gudmundsson, A.T, and Kjartansson, H., 1996: *Earth in action*. Vaka-Helgafell, Reykjavík, 166 pp.

Hardarson, B.S., Einarsson, G.M., Franzson, H., and Gunnlaugsson, E., 2009: Volcano-tectonic-geothermal interaction at the Hengill triple junction, SW Iceland. *Geothermal Resources Council, Transactions, 33,* 49-54.

Jakobsson, S.P, Jónasson, K, and Sigurdsson, I.A., 2008: The three igneous rock series of Iceland. *Jökull, 58,* 117-138.

Jóhannesson, H. and Saemundsson, K., 1998: *Geological map of Iceland 1:500.000* (2nd edition). Náttúrufraedistofnun Íslands and Landmaelingar Íslands.

Jónsson, J., 1989: *Hveragerdi and surroundings, geological overview.* Rannsóknarstofnunin Nedri Ás, report 50 (in Icelandic), 56 pp and map.

Khodayar, M., Ólafsson, G.E., Gudnason, J., and Björnsson, S., 2008: *Preliminary observations of surface ruptures and geothermal manifestations associated with the 29 May 2008 earthquakes, South Iceland Seismic Zone*. ÍSOR – Iceland GeoSurvey, Reykjavík, report ÍSOR-08060, 10 pp.

Kristjánsson, B.R., and Fridriksson, Th., 2003: *State Horticultural School, Reykir in Ölfus, geothermal map*. ISOR - Iceland GeoSurvey, Reykjavík, report 2003-01 (in Icelandic), 4 pp.

Kyagulanyi, D., 1996: Geothermal exploration in the Hveragerdi-Graendalur area, SW-Iceland. Report 8 in: *Geothermal training in Iceland 1996*. UNU-GTP, Iceland, 161-176.

Malik, A.H., 1996: Geothermal exploration of Saudá valley north of Hveragerdi, SW-Iceland. Report 9 in: *Geothermal training in Iceland 1996*. UNU-GTP, Iceland, 177-195.

Munasinghe, M.M.T.N.B., 2013: Geothermal exploration in Gufudalur, Hveragerdi, SW-Iceland. Report 21 in: *Geothermal training in Iceland 2013*. UNU-GTP, Iceland, 477-500.

Ragnarsson Á., 2015: Geothermal development in Iceland 2010-2014. *Proceedings of the World Geothermal Congress 2015, Melbourne, Australia*, 15 pp.

Saemundsson, K., 1967: Vulkanismus und Tektonik des Hengill-Gebietes in Sudwest-Island. *Acta Nat. Isl., II-7, (in German)*, 195 pp.

Saemundsson, K., 1979*:* Outline of geology of Iceland. *Jökull, 29*, 7-28.

Saemundsson, K., 1993a: *Hveragerdi - geothermal activity*. Orkustofnun, Reykjavík, report KS-93/20, 33 pp.

Saemundsson, K., 1993b: *Geothermal map of Hveragerdi and Reykir.* Orkustofnun, Reykjavík, report JHD-JFR8716, 54 pp.
Saemundsson, K., 1995a: *Geological map of the Hengill area 1:50,000*. Orkustofnun, Reykjavík.

Saemundsson, K., 1995b: *Geothermal and hydrothermal map of the Hengill area, 1:25,000.* Orkustofnun, Reykjavík.

Saemundsson, K., and Arnórsson, S., 1971: *A report on well* Asi-1 *at Ölfusborgir, Ölfus.* Orkustofnun, Reykjavík, report (in Icelandic), 9 pp and figs.

Saemundsson, K., Axelsson, G., and Steingrímsson, B., 2009: Geothermal systems in global perspective. *Proceedings of a "Short Course on Surface Exploration for Geothermal Resources", organized by UNU-GTP and LaGeo, Santa Tecla, El Salvado*r, UNU-GTP, SC-09, 16 pp.

Saemundsson, K., and Einarsson, S., 1980: *Geological map of Iceland, sheet 3, SW-Iceland* (2nd ed.). Museum of Natural History and Geodetic Survey, Reykjavík, Iceland.

Saemundsson, K., and Fridleifsson, G.Ó., 1992: *The Hveragerdi central volcano, geological description.* Orkustofnun, Reykjavík, report OS-92063/JHD-35 B (in Icelandic), 25 pp.

Saemundsson, K., and Fridleifsson. G.Ó., 1996: The Hveragerdi central volcano. An extended English abstract from Saemundsson, K., and Fridleifsson, G.Ó., 1992: *The Hveragerdi central volcano, geological description.* Orkustofnun, Reykjavik, report GÓF-KS-96/03, 10 pp.

Saemundsson, K., and Kristinsson, S.G., 2005: *Hveragerdi, temperature measurements in soil and fractures.* ÍSOR - Iceland GeoSurvey, Reykjavík, report ISOR-2005/041 (in Icelandic), 16 pp + 2 maps.

Thorbjörnsson, D., Saemundsson, K., Kristinsson, S.G., Kristjánsson, B.R, and Ágústsson, K, 2009: *Southern lowland earthquakes 29th May, 2008, effect of groundwater level, geothermal activity and fractures*. ÍSOR – Iceland GeoSurvey, Reykjavík, report ÍSOR-2009/028 (in Icelandic), 42 pp.

Thórdarson, T., 2012: Outline of geology of Iceland. *Chapman Conference 2012*, *Selfoss, Iceland*, 15 pp.

Walker, C.L., 1992: *The volcanic history and geochemical evolution of the Hveragerdi region, SW Iceland.* University of Durham, Durham, UK, PhD thesis, 356 pp.

Wangombe, P.W., 1987: *Mapping at Grensdalur-Reykjadalur area, Hveragerdi, SW-Iceland*. UNU-GTP, Iceland, report 15, 26 pp.

APPENDIX I: XRD analysis of alteration samples taken in the study area

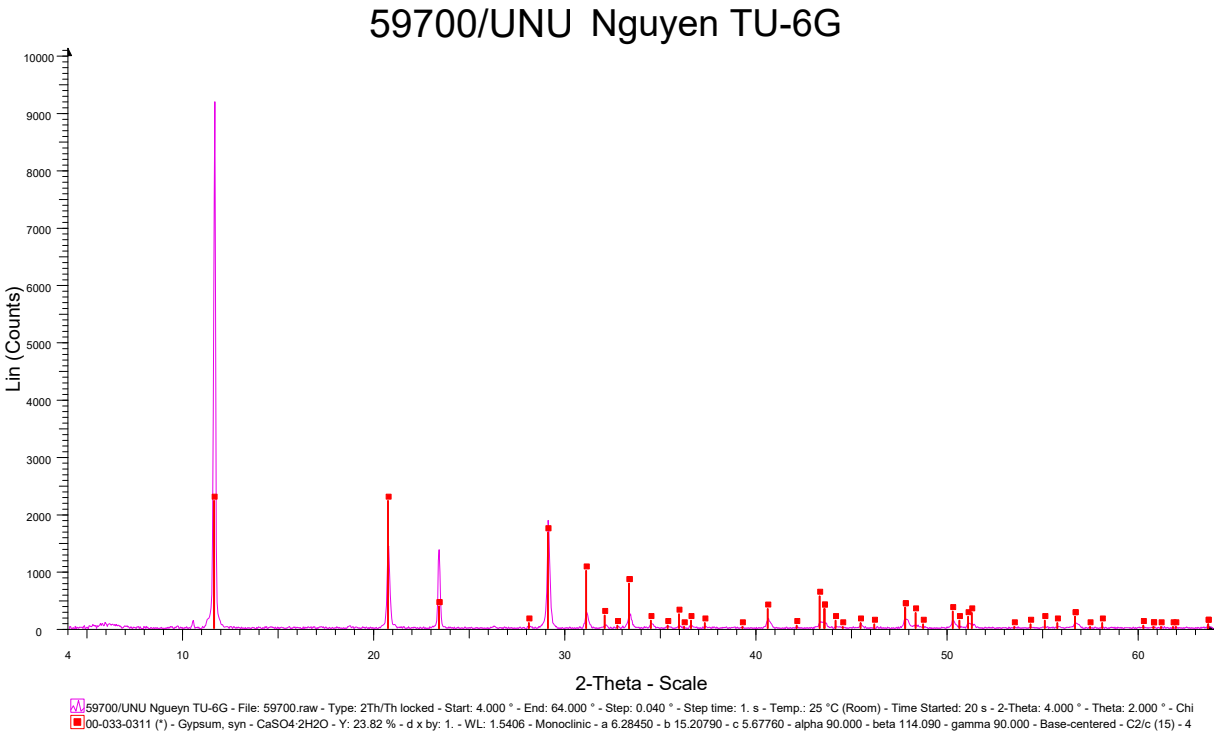

FIGURE 1: XRD graph showing the presence of gypsum in sample TU 6 collected in mud pool at location no. 3A

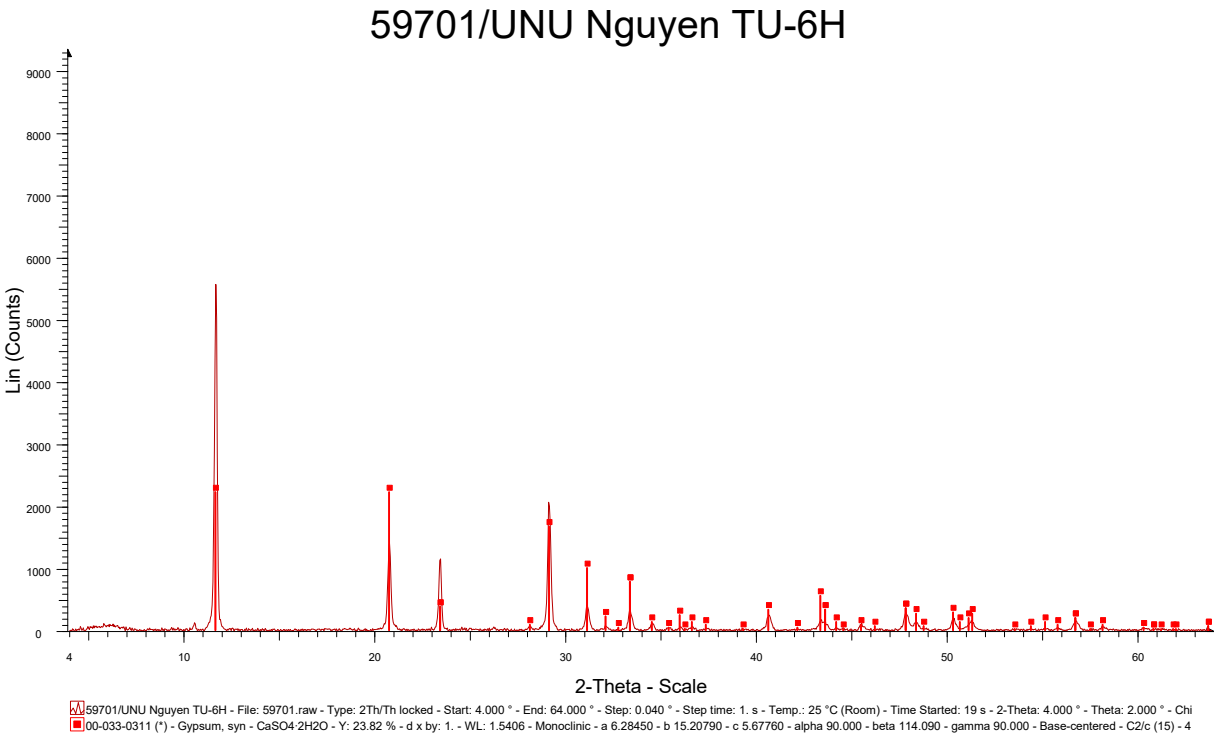

FIGURE 2: XRD graph showing the presence of gypsum in sample TU 6 collected in mud pool at location no. 3A

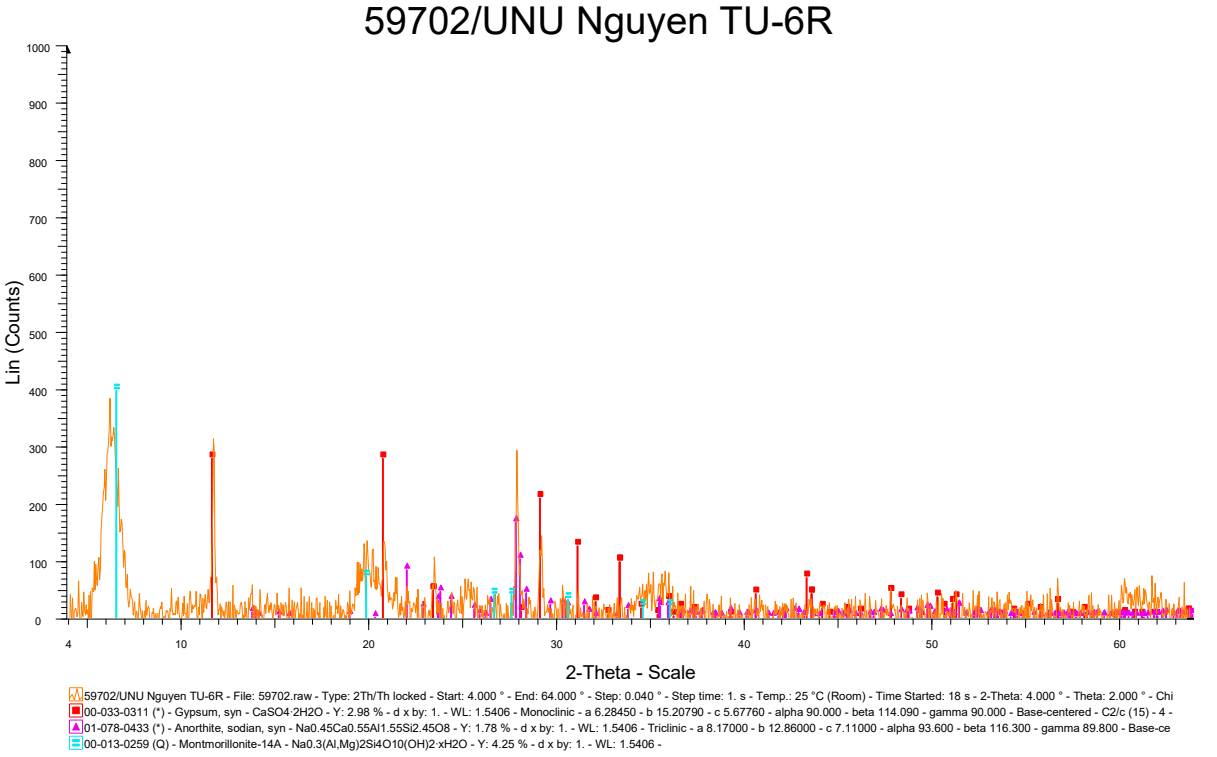

FIGURE 3: XRD graph showing the presence of gypsum, anorthite and montmorillonite (smectite) minerals in sample TU 6 collected in fumarole at location no. 3A

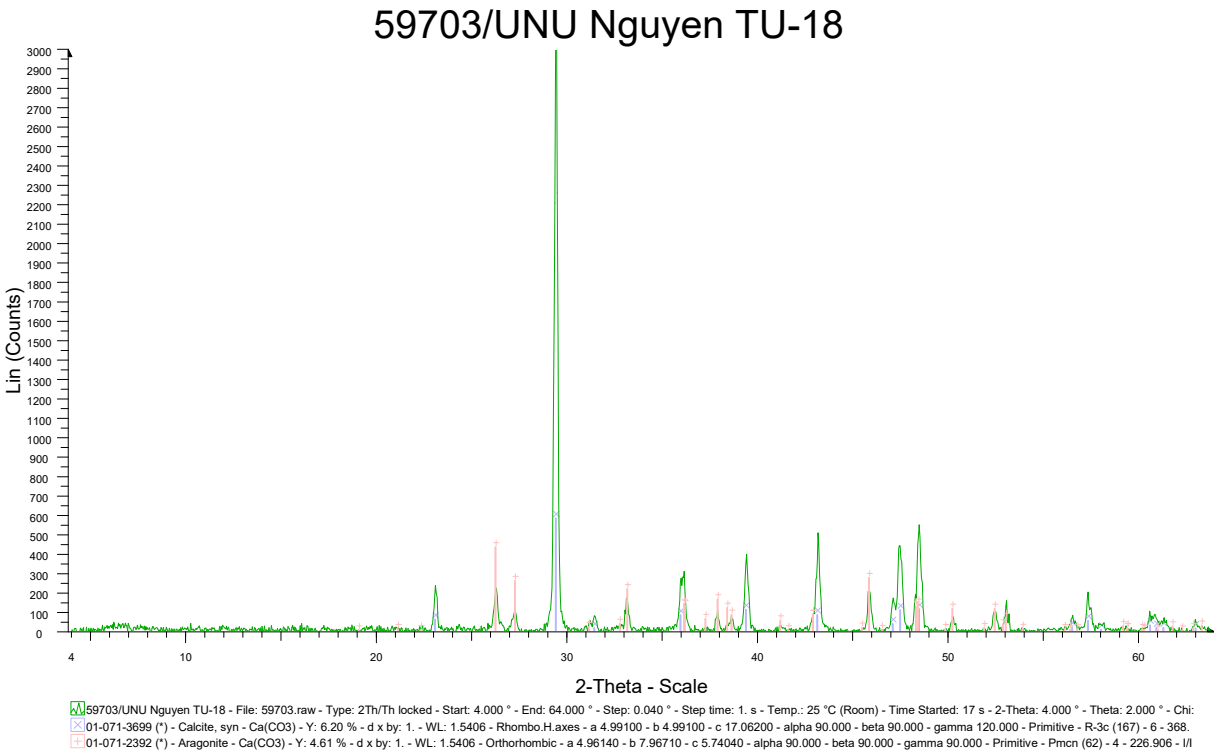

FIGURE 4: XRD graph showing the presence of calcite and aragonite in sample TU 18 collected in fumarole at location no. 3A